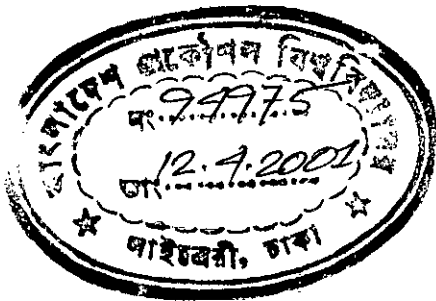


MODELING OF FLAME PROPAGATION IN LAMINAR BIOGAS-AIR PREMIXTURE

By

MD. MIZANUZZAMAN

B.Sc. Engg. (Mech.)



A Thesis

Submitted to the Department of Mechanical Engineering in partial fulfillment of the requirements
For

The degree of Master of Science in Mechanical Engineering

BANGLADESH UNIVERSITY OF ENGINEERING AND TECHNOLOGY,
Dhaka, Bangladesh.
January, 2001



RECOMMENDATION OF THE BOARD OF EXAMINERS

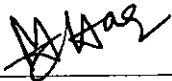
The thesis titled

MODELING OF FLAME PROPAGATION IN LAMINAR BIOGAS-AIR PREMIXTURE

submitted by

Md. Mizanuzzaman, Roll No - 9610007(F), Session : 1995 - 96 - 97

to the Mechanical Engineering Department of Bangladesh University of Engineering and Technology has been accepted as satisfactory for partial fulfillment of the requirements for the degree of Master of Science in Mechanical Engineering on January 15, 2001.



Dr. Md. Zahurul Haq
Assistant Professor
Department of Mechanical Engineering
BUET, Dhaka - 1000, Bangladesh

Chairman
(supervisor)



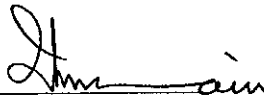
Dr. Md. Abdur Rashid Sarkar
Professor and Head of the
Department of Mechanical Engineering
BUET, Dhaka - 1000, Bangladesh

Member
(Ex - officio)



Dr. Md. Ehsan
Assistant Professor
Department of Mechanical Engineering
BUET, Dhaka - 1000, Bangladesh

Member

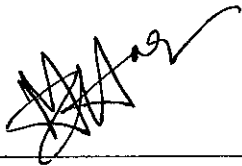


Dr. A. K. M. Iqbal Hussain
Professor and Head of the
Energy and Environment center
Islamic Institute of Technology (IIT)
The Organisation of the Islamic Conference (OIC)
Board Bazar, Gazipur - 1704

Member
(External)

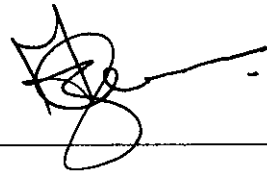
CERTIFICATE OF RESEARCH

This is to certify that the work presented in the dissertation is the outcome of the investigation carried out by the author under the supervision of Dr. Md. Zahurul Haq, Assistant Professor, Department of Mechanical Engineering, Bangladesh University of Engineering and Technology (BUET), Dhaka, Bangladesh and that it has not been submitted anywhere for the award of any degree or diploma.



Supervisor

Dr. Md. Zahurul Haq



Author

Md. Mizanuzzaman

Abstract

In view of the energy crisis and emission problems, alternative fuels are promising substitute to the conventional petroleum based fuels, specially in internal combustion engines. Among these, bio-gas is an attractive substitute to conventional petroleum fuels. They have the advantage of being very cheap and are renewable in nature, and thereby not contributing to the net atmospheric concentration of the green house gas, carbon-di-oxide. However there is a dearth of bio-gas combustion data. Various data regarding combustion of methane is available. So it is essential and possible to model the bio-gas combustion as it contains a blend of methane, carbon-di-oxide, oxygen and very less amount of organic/non-organic elements. Reaction mechanism for methane and bio-gas combustion are essentially same and therefore might provide useful data required for the optimization of bio-gas air combustion.

In the present study, heat release and equilibrium composition of methane and bio-gas air premixture are studied numerically for different initial conditions of composition and pressure. Laminar flame structure and burning velocities are also modeled. Results obtained from this study emphasizes the importance of composition and pressure in the combustion process and draws some recommendations for the optimization of combustion bio-gas of different composition.

Acknowledgments

The author wishes to express his sincerest as well as heartfelt gratitude and indebtedness to his thesis supervisor Dr. Md. Zahurul Haq, Assistant Professor, Department of Mechanical Engineering, BUET, Dhaka, for his guidance, supervision and moral support throughout the entire period of the thesis work. His initiative, encouragement, patience and invaluable suggestions are very gratefully acknowledged. It is a great pleasure for working with him and learning the different facets of research. Specially grateful to him for showing the way of go inside the beauty of CFD.

The author wishes to express thanks and regards to Dr. Md. Abdur Rashid Sarkar, Professor and Head of the Department of Mechanical Engineering, BUET, Dhaka, for his encouragement and cooperation to complete this work successfully.

The author also thanks his friends, family and relatives, those who shared the troubles.

TO
My Parents

Table of Contents

Abstract	iv
Acknowledgments	v
List of Tables	ix
List of Figures	x
Chapter 1. Introduction	1
1.1 Energy and Environmental Problems	1
1.2 Present Status of Alternative Fuels	2
1.3 Natural Gas and Bio-gas as Alternative Fuels	3
1.4 Scope of the Thesis	4
Chapter 2. Thermodynamics and Thermochemistry of Bio-gas Air Combustion	5
2.1 Ideal Gas Equation of State	5
2.2 Combustion Stoichiometry	6
2.3 Thermodynamic Properties	8
2.4 Heat Release from Biogas Combustion	9
2.5 Chemical Equilibrium and Adiabatic Flame Temperature	12
2.6 Estimation of Heat Release	15
2.7 Estimation of Chemical Equilibrium Composition	16
2.7.1 Estimation of Product Composition at Low Tempera- ture	17

2.7.2	Estimation of T_{ad} and Product Compositions	18
2.8	Results and Discussion	19
Chapter 3.	Bio-gas Air Flame Structure and Laminar Burning Ve-	
	locities	35
3.1	Modeling of Premixed Adiabatic Laminar Flame	36
3.2	Computation Technique and Program Structure	39
3.3	Problem Solution, Convergency and Consistency of Solution .	41
3.4	Results and Discussions	42
Chapter 4.	Conclusions	58
Appendix A.	Typical Output from EQUIL Code	60
Appendix B.	Methane Reaction Pathways	62
Appendix C.	GRI-Mech 1.2: Methane Reaction Mechanism	64
Appendix D.	Input of PREMIX INPUT	74
References	76

List of Tables

2.1	Coefficients of species thermodynamic properties	10
2.2	Low temperature combustion products, ν_j (moles/mole of air) . . .	18

List of Figures

2.1	Heating values for a bio-gas at different values of β	23
2.2	Specific Energy and Energy Density for bio-gas air premixture as a function of ϕ	24
2.3	Combustion product equilibrium composition of $[CO_2]$, $[CO]$, $[H_2O]$, $[H_2]$, $[N_2]$ and $[O_2]$ as a function of ϕ at different temperature.	25
2.4	Dissociation of CO_2 , H_2 and O_2 as a function of temperature.	26
2.5	Mole fractions of equilibrium combustion products and adiabatic temperatures of methane-air premixture as a function of ϕ	27
2.6	Variation of T_{ad} 's as a function of ϕ for different values of β at two initial pressures of 0.1 and 1.0 MPa.	28
2.7	Variation of ρ 's as a function of ϕ for different values of β at two initial pressures of 0.1 and 1.0 MPa.	29
2.8	Variation of $[O_2]$'s as a function of ϕ for different values of β at two initial pressures of 0.1 and 1.0 MPa.	30
2.9	Variation of $[CO_2]$'s as a function of ϕ for different values of β at two initial pressures of 0.1 and 1.0 MPa.	31
2.10	Variation of $[CO]$'s as a function of ϕ for different values of β at two initial pressures of 0.1 and 1.0 MPa.	32
2.11	Variation of $[H_2]$'s as a function of ϕ for different values of β at two initial pressures of 0.1 and 1.0 MPa.	33
2.12	Variation of $[H_2O]$'s as a function of ϕ for different values of β at two initial pressures of 0.1 and 1.0 MPa.	34

3.1	Structure of the adiabatic, one-dimensional, freely propagating planar premixed flame at increasingly detailed levels of description: (a) hydrodynamic level; (b) transport level; and (c) reaction level.	45
3.2	Relationship of PREMIX to CHEMKIN and TRANFIT; and the associated input and output files.	46
3.3	Test of convergence of solution using PREMIX.	47
3.4	Example of comparison of results of PREMIX with RUN-1DL.	47
3.5	Composition, temperature profile of one-dimensional, freely propagating methane-air mixture.	48
3.6	Variation of temperature with axial distance, for different stoichiometry, composition of bio-gas and pressure.	49
3.7	Variation of $[CH_4]$ with axial distance, for different stoichiometry, composition of bio-gas and pressure.	50
3.8	Variation of $[O_2]$ with axial distance, for different stoichiometry, composition of bio-gas and pressure.	51
3.9	Variation of $[H_2O]$ with axial distance, for different stoichiometry, composition of bio-gas and pressure.	52
3.10	Variation of $[CO_2]$ with axial distance, for different stoichiometry, composition of bio-gas and pressure.	53
3.11	Variation of $[CO]$ with axial distance, for different stoichiometry, composition of bio-gas and pressure.	54
3.12	Variation of $[H_2]$ with axial distance, for different stoichiometry, composition of bio-gas and pressure.	55
3.13	Variation of mass flux, \dot{m} , with axial distance, for different stoichiometry, composition of bio-gas and pressure.	56
3.14	Laminar burning velocities plotted against (a) ϕ , (b) β at different pressure.	57
B.1	High temperature reaction pathway diagram for methane.	62
B.2	Low temperature reaction pathway diagram for methane.	63

List of Symbols

a_{ij}	NASA Coefficients for species thermodynamic properties
A	Pre-exponential factor (Eq ⁿ . 3.8)
b	Temperature exponent (Eq ⁿ . 3.8)
c_p	Specific heat at constant pressure (kJ/kg-K)
D_{ij}	Binary diffusion coefficients for pairs of species (Eq ⁿ . 3.5)
E_A	Activation energy, kJ/kg (Eq ⁿ . 3.8)
ED	Energy density (kJ/m ³ -mix)
$(F/A)_{act}$	Actual fuel-air ratio
$(F/A)_{stoic}$	Stoichiometric fuel-air ratio
G	Gibbs energy (kJ/kmol)
h_{fg}	Latent heat of vaporization
H	Enthalpy (kJ/kmol)
HHV	Higher Heating Value (kJ/kg-fuel)
k_f	Forward rate of coefficient (Eq ⁿ . 3.8)
k_{mix}	Thermal conductivity of mixture (Eq ⁿ . 3.7)
K_p	Chemical equilibrium constant (Eq ⁿ . 2.37)
LHV	Lower Heating Value (kJ/kg-fuel)
\dot{m}	Mass flux (defined in Eq ⁿ . 3.1)
m_i	Mass of species, i
P	Pressure
P_j	Product species
P_u	Unburned initial pressure
R	Specific gas constant (kJ/kg-K)

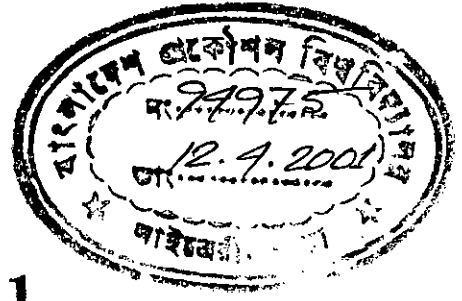
R_i	Reactant species
R_u	Universal gas constant (8.314 kJ/kmol-K)
S	Entropy (kJ/kmol-K)
SE	Specific energy (kJ/kg-mix)
T_{ad}	Adiabatic temperature (K)
T_{ig}	Ignition temperature (K)
u_l	Laminar Burning velocity (m/s)
V	Volume
X_i	Mole fraction of species, i
Y_i	Mass fraction of species, i

Greek letters

α	Thermal diffusivity
α_{mix}	Thermal diffusivity of mixture (Eq ⁿ . 3.7)
β	% of CO ₂ (by volume) in Biogas
ε	Molar fuel-air ratio
ν_i	Stoichiometric coefficient of reactant species, i
$\nu_{i,diff}$	Diffusion velocity (Eq ⁿ . 3.4)
$\nu_{i,diff,T}$	Force diffusion velocity (Eq ⁿ . 3.4)
$\nu_{i,diff,P}$	Pressure diffusion velocity (Eq ⁿ . 3.4)
$\nu_{i,diff,T}$	Thermal diffusion velocity (Eq ⁿ . 3.6)
$\nu_{i,diff,X}$	Ordinary diffusion velocity (Eq ⁿ . 3.5)
ν_j	Stoichiometric coefficient of product species, j
ρ	Density
ϕ	Equivalence ratio
$\dot{\omega}_i$	Mass production rate of species, i (Eq ⁿ . 3.2)

Additional Symbols

[A]	Mole fraction of species, A
Π	Multiplication notation
Δ	Difference notation
Σ	Summation notation



Chapter 1

Introduction

There is a continuing demand for increased combustion efficiency and a deepening concern over problems related to the energy, economy and environment. All of these have, during past decades, stimulated a tremendous burst of interest and research activities in the field of combustion of both conventional and alternative fuels. Now a days, major share of energy production is linked to combustion, directly or indirectly. Good combustion results in more useful energy at low cost and causes less pollution. Alternative/renewable fuels are less polluting and their net contribution to the global warming gas (carbon-di-oxide) is zero. In the present study, combustion of natural gas, which is abundant in Bangladesh, and bio-gas, which is cheap and renewable in nature, are numerically studied to give insight into the burning process required for their optimum and efficient utilization.

1.1 Energy and Environmental Problems

The end of the era of 'cheap energy' has been proclaimed frequently ever since, and predictions of future energy patterns and policies have featured in all forms of discussion, debate and dissemination. The vital nature of an assured supply of energy, at realistic costs has now been recognized for the continuation and improvement of our lifestyle. Because of the possible demise of some conventional

fossil fuels, many research programs are directed towards the long-term harnessing of alternative sources of energy including wind, waves, tides, geo-thermal, solar radiation and nuclear fusion in addition to the alternative fuels. Ever increasing energy demand can only be met by means of fuels derived from alternative, replenish-able sources, also by efficient conversion of conventional fuels (Goodger 1980).

In recent days, combustion of conventional fuel are under strict scrutiny because of the emissions caused, e.g. unburned and partially burned hydrocarbons, nitrogen oxides, carbon monoxide, sulphur oxides, and particulate matters in various forms. These cause concerns related to specific health hazards, smogs, acid rain, global warming, and ozone depletion. Now-a-days, combustion generated emission are subjected to strict governmentally imposed emission standards for selected compounds in the products (De Nevers 2000). Low emissions can be achieved by a combination of fuel selection and preparation, combustion system design, and treatment of the products of combustion.

There are challenging engineering trade-off between low emissions, high efficiency and low cost. Recently, global warming has become a widespread concern. Carbon dioxide levels in the global atmosphere are increasing at an accelerated rate, and hydrocarbon fuel combustion is blamed as the major contributor to the greenhouse effect. The world-wide pressure for population growth in fuel consumption and CO_2 emission is tremendous. So concern over the environmental issues may limit the use of fossil fuels in the future. Renewable energy sources such as wind, solar, tidal, geothermal energy, and alternative fuels may become more important in the future.

1.2 Present Status of Alternative Fuels

The extent of global fossil fuel reserves is subject to debate. With the present world production and consumption rates of petroleum based fuels, it is approximated these resources will be depleted in foreseeable future. So with increasing

the demand with time, reserves will be decreasing. This put an extra emphasis on the search for alternative energy sources and also for better combustion process.

Alternative fuels are inherently cleaner than petroleum derived fuels. Several candidate alternative fuels exist that include bio-gas, bio-diesel, rice bran oils, vegetable oils, synthetic fuels, alcohols, municipal wastes etc. When used with advanced engine and emission control technologies, alternative fuels burn efficiently and release fewer emissions from incomplete combustion. Advanced combustion and emission control technology requires combustion data with certain degree of detailing. Data for conventional fuels are available, however, there is a dearth of combustion data for alternative fuels. Generation of experimental data is very expensive, and therefore more emphasis is given, now-a-days, on modeled results for combustion of non-conventional fuels.

1.3 Natural Gas and Bio-gas as Alternative Fuels

Bio-gas is a very potential alternative fuel candidate. Natural gas is used world- wide but its reserve is limited. So, as a renewable fuel bio-gas came front, and its production as well as utilization increases day by day. Therefore, it is important to study bio-gas combustion to have better insight into the combustion process itself for its optimum utilization.

Methane the major component of natural gas as well as bio-gas. Methane is the simplest of the hydrocarbon series and modeled data for the combustion are very consistent with the experimental results. Same reaction mechanism can be used to model bio-gas combustion. Bio-gas is a colorless combustible gas which produced by fermentation of cellulose material (woody and nonwoody), manure or cowdung. Methane and CO_2 constitutes about 95% of biogas and trace organic/non-organic elements of variable compositions. Moreover, the amount of CH_4 and CO_2 in bio-gas varies with different sources of origin (Goodger 1980). The variation in its affects combustion process and the heat release rates. Therefore, premixed combustion of bio-gas requires detailed study.

1.4 Scope of the Thesis

The present thesis comprises a numerical study of freely-propagating, one-dimensional, planar, adiabatic premixed flame propagation in methane, bio-gas and air premixture. The effect of the concentration of CO_2 in bio-gas mixtures are studied at different equivalence ratios at 300 K, at initial pressures of 0.1 and 1.0 MPa. In the present study, mole fraction of CO_2 are denoted by β and study is carried out for $\beta = 0, 0.1, 0.2, 0.3, 0.4$ and 0.5 .

In Chapter 2, heat release rate and the equilibrium temperature and compositions are the focus of study, while burning velocities and laminar flame structure are reported in Chapter 3. Chapter 4 draws conclusions from the work and makes some recommendations.

Chapter 2

Thermodynamics and Thermochemistry of Bio-gas Air Combustion

In view of the prevailing energy crisis and pollution problems, bio-gas is a promising substitute to conventional fuels. Methane and carbon-di-oxide constitute about 95% of bio-gas, while its composition varies from different sources (Goodger 1980). Bari *et al.* (1994) reported that the available power is reduced in diesel engines when using bio-gas with different concentration of carbon-di-oxide. The present chapter reports the effect of carbon-di-oxide concentration in bio-gas combustion.

2.1 Ideal Gas Equation of State

Ideal gas equation of state provides the basic relationship among pressure, P , temperature, T , and density, ρ , of ideal gas species and their mixtures. Hence,

$$P = \rho RT \quad (2.1)$$

where, specific gas constant, R , is related to Universal gas constant, R_u (=8.314 kJ/kmol-K) and the gas molecular weight, M , by

$$R = \frac{R_u}{M} \quad (2.2)$$

For multicomponent ideal gas mixtures of n species, the mole fraction, X_i , and mass fraction, Y_i , of species, i , are defined as

$$X_i \equiv \frac{N_i}{X_1 + X_2 + \cdots + X_n} = \frac{N_i}{\sum N_i} \quad (2.3)$$

$$Y_i \equiv \frac{m_i}{m_1 + m_2 + \cdots + m_n} = \frac{m_i}{\sum m_i} \quad (2.4)$$

where,

N_i = Number of moles of species, i

m_i = mass of species, i

and, by definition,

$$\sum X_i = 1 \quad \text{and} \quad \sum Y_i = 1 \quad (2.5)$$

Values of X_i and Y_i are related by

$$Y_i = \frac{M_i}{M_{mix}} X_i \quad (2.6)$$

where, the mean molecule weight of the mixture, M_{mix} , is given by Borman and Ragland (1998) as:

$$M = \sum M_i X_i = \frac{1}{\sum (Y_i/M_i)} \quad (2.7)$$

2.2 Combustion Stoichiometry

General stoichiometric reaction can be written as:



where,

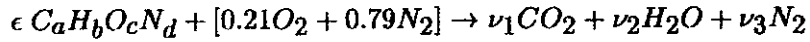
ν_i = Stoichiometric coefficient of reactant species, i

ν_j = Stoichiometric coefficient of product species, j

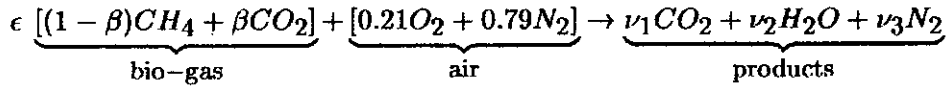
R_i = Reactant species, i

P_j = Product species, j

In general, fuels contain carbon, hydrogen, oxygen and nitrogen, in addition to some minor species. When fuel is burned to completion with a stoichiometric amount of air (assuming that air contains 21% O_2 and 79% N_2 by volume), general stoichiometric reaction can be written as:



where, ϵ = molar fuel-air ratio. Hence, the combustion product is assumed to contain only CO_2 , H_2O and N_2 , without any dissociation. Biogas combustion reaction with stoichiometric amount of air can be written as:



In any chemical reaction, atoms are conserved. Hence, by atom balances:

$$C : \epsilon(1 - \beta + \beta) = \nu_1 \quad (2.9)$$

$$H : 4\epsilon(1 - \beta) = 2\nu_2 \quad (2.10)$$

$$O : 2\epsilon\beta + 0.42 = 2\nu_1 + \nu_2 \quad (2.11)$$

$$N : 1.58 = 2\nu_3 \quad (2.12)$$

and, solution of Eqns.2.9-2.12 yield,

$$\epsilon = \frac{0.105}{1 - \beta} \quad (2.13)$$

Stoichiometric fuel-air ratio by mass, $(F/A)_{stoic}$, can be written as:

$$\left(\frac{F}{A}\right)_{stoic} = \left(\frac{m_{fuel}}{m_{air}}\right)_{stoic} = \epsilon \frac{M_{fuel}}{M_{air}} = \epsilon \frac{(1 - \beta)M_{CH_4} + \beta M_{CO_2}}{0.21M_{O_2} + 0.79M_{N_2}} \quad (2.14)$$

The mole and mass fraction of a stoichiometric mixture are given by Ferguson (1960) as:

$$X_{stoic} = \frac{\epsilon}{1 + \epsilon} \quad (2.15)$$

$$Y_{stoic} = \frac{(F/A)_{stoic}}{1 + (F/A)_{stoic}} \quad (2.16)$$

Fuel-air equivalence ratio, ϕ , is commonly used to indicate quantitatively whether a fuel-oxidizer mixture is rich, lean or stoichiometric and is defined as

$$\phi = \frac{(F/A)_{act}}{(F/A)_{stoic}} = \frac{(A/F)_{stoic}}{(A/F)_{act}} \quad (2.17)$$

Hence,

$$\phi \begin{cases} < 1 & \text{lean mixture (excess } O_2 \text{ is present)} \\ = 1 & \text{stoichiometric mixture (correct amount of } O_2 \text{ is present)} \\ > 1 & \text{rich mixture (shortage of } O_2 \text{ to complete combustion)} \end{cases}$$

2.3 Thermodynamic Properties

Heat release from combustion, equilibrium composition and temperature are estimated using thermodynamic properties of the gases. Mixture properties are estimated from pure species properties via some mixture averaging rules. The thermodynamic and thermo-chemical data are widely represented as two sets of polynomial coefficients for each species. These polynomials are widely known as the NASA polynomials (Burcat and McBride 1997). The first set reproduces data above 1000 K, the second set below 1000 K. The same 1000 K value is reproduced by both sets. The following standard molar thermodynamic functions can be obtained from the polynomial coefficients:

$$\frac{C_{P,i}}{R_u} = a_1 + a_2 T + a_3 T^2 + a_4 T^3 + a_5 T^4 \quad (2.18)$$

$$\frac{H_{T,i}}{R_u T} = a_1 + a_2 \frac{T}{2} + a_3 \frac{T^2}{3} + a_4 \frac{T^3}{4} + a_5 \frac{T^4}{5} + \frac{a_6}{T} \quad (2.19)$$

$$\frac{S_{T,i}}{R_u} = a_1 \ln T + a_2 T + a_3 \frac{T^2}{2} + a_4 \frac{T^3}{3} + a_5 \frac{T^4}{4} + a_7 \quad (2.20)$$

$$\frac{G_{T,i}}{R_u T} = \frac{H_{T,i}}{R_u T} - \frac{S_{T,i}}{R_u} = a_1(1 - \ln T) - a_2 \frac{T}{2} - a_3 \frac{T^2}{6} - a_4 \frac{T^3}{12} - a_5 \frac{T^4}{20} + \frac{a_6}{T} - a_7 \quad (2.21)$$

The coefficients, a_{ij} , are taken from Burcat and McBride (1997) and values of these coefficients of some major species are reported in Table 3.1. The mixture properties are defined as the mole-fraction-weighted averages (e.g. C_p , H , S , G etc.), given by

$$C_p = \sum X_i C_{p_i}, \quad H = \sum X_i H_i, \quad S = \sum X_i S_i \quad \text{and} \quad G = \sum X_i G_i \quad (2.22)$$

,or, as the mass-fraction-weighted averages (e.g. c_p , h , s , g etc.), given by

$$c_p = \sum Y_i c_{p_i}, \quad h = \sum Y_i h_i, \quad s = \sum Y_i s_i \quad \text{and} \quad g = \sum Y_i g_i \quad (2.23)$$

2.4 Heat Release from Biogas Combustion

Combustion is a mass and energy conversion process during which chemical bond energy is transformed to thermal energy. Fuels react with oxygen of air to form products such as CO_2 and H_2O with lower chemical bond energy than the reactants, and therefore release heat (Goodger 1980). Heat available from the combustion of unit mass of fuel in a stoichiometric mixture is defined as heating value. Two heating values are recognized by namely:

1. HHV (Higher Heating Value), and
2. LHV (Lower Heating Value).

Table 2.1. Coefficients of species thermodynamic properties

Species	T range, K	a_{i1}	a_{i2}	a_{i3}	a_{i4}	a_{i5}	a_{i6}	a_{i7}
CO ₂	1000-5000	0.44608(+1)	0.30982(-2)	-0.12393(-5)	0.22741(-9)	-0.15526(-13)	-0.48961(+5)	-0.98636(0)
	300-1000	0.24008(+1)	0.87351(-2)	-0.66071(-5)	0.20022(-8)	0.63274(-15)	-0.48378(+5)	0.96951(+1)
H ₂ O	1000-5000	0.27168(+1)	0.29451(-2)	-0.80224(-6)	0.10227(-9)	-0.48472(-14)	-0.29906(+5)	0.66306(+1)
	300-1000	0.40701(+1)	-0.11084(-2)	0.41521(-5)	-0.29637(-8)	0.80702(-12)	-0.30280(+5)	-0.32270(0)
CO	1000-5000	0.29841(+1)	0.14891(-2)	-0.57900(-6)	0.10365(-9)	-0.69354(-14)	-0.14245(+5)	0.63479(+1)
	300-1000	0.37101(+1)	-0.16191(-2)	0.36924(-5)	-0.20320(-8)	0.23953(-12)	-0.14356(+5)	0.29555(+1)
H ₂	1000-5000	0.31002(+1)	0.51119(-3)	0.52644(-7)	-0.34910(-10)	0.36945(-14)	-0.87738(+3)	-0.19629(+1)
	300-1000	0.30574(+1)	0.26765(-2)	-0.58099(-5)	0.55210(-8)	-0.18123(-11)	-0.98890(+3)	-0.22997(+1)
O ₂	1000-5000	0.36220(+1)	0.73618(-3)	-0.19652(-6)	0.36202(-10)	-0.28946(-14)	-0.12020(+4)	0.36151(+1)
	300-1000	0.36256(+1)	-0.18782(-2)	0.70555(-5)	-0.67635(-8)	0.21556(-11)	-0.10475(+4)	0.43053(+1)
N ₂	1000-5000	0.28963(+1)	0.15155(-2)	-0.57235(-6)	0.99807(-10)	-0.65224(-14)	-0.90586(+3)	0.61615(+1)
	300-1000	0.36748(+1)	-0.12082(-2)	0.23240(-5)	-0.63218(-9)	-0.22577(-12)	-0.10612(+4)	0.23580(+1)
OH	1000-5000	0.29106(+1)	0.95932(-3)	-0.19442(-6)	0.13757(-10)	0.14225(-15)	0.39354(+4)	0.54423(+1)
NO	1000-5000	0.31890(+1)	0.13382(-2)	-0.52899(-6)	0.95919(-10)	-0.64848(-14)	0.98283(+4)	0.67458(+1)
O	1000-5000	0.25421(+1)	-0.27551(-4)	-0.31028(-8)	0.45511(-11)	-0.43681(-15)	0.29231(+5)	0.49203(+1)
H	1000-5000	0.25(+1)	0.0	0.0	0.0	0.0	0.25472(+5)	-0.46012(0)

Higher heating values are obtained when all the water formed by combustion are in liquid phase; for lower heating value all the water formed by combustion is in vapor phase. The higher heating value exceeds the lower heating value by the energy that would be required to vaporize the liquid formed. Discrepancy between the HHV and LHV depends on the amount of hydrogen present in the fuel. The two heating values at constant pressure are related by:

$$HHV = LHV + \left[\frac{m_{H_2O}}{m_{fuel}} \right] h_{fg} \quad (2.24)$$

where,

$$\frac{m_{H_2O}}{m_{fuel}} = \text{mass of } H_2O \text{ produced per unit mass of fuel burned, and}$$

$$h_{fg} = \text{latent heat of vaporization of water at } 25^\circ C (= 2442 \text{ kJ/Kg})$$

Lower heating value (LHV) are widely used as combustion process temperature is high and water products are in vapor phase. Higher heating value (HHV) gives an indication to the possible maximum or gross amount of energy.

Practical combustion processes are not essentially stoichiometric, and are maintained in a band of equivalence ratios, as set in the design condition. Hence, heat available from the combustion of mixture of different fuels at different equivalent ratio's are different. Heat availability from a given amount of charge (air and fuel mixture) might be defined in two ways:

1. Specific Energy, $SE_{\beta\phi}$: heat available from unit mass of mixture.
2. Energy Density, $ED_{\beta\phi}$: heat available from unit volume of mixture.

Both of these quantities are important as these values give the amount of heat release from a premixture, former one on mass basis and the later one on volume basis.

2.5 Chemical Equilibrium and Adiabatic Flame Temperature

In many instances, the level of temperature achieved during combustion is a measure of the gross efficiency of the overall conversion of stored chemical energy. Experimental methods of determination of combustion temperature are available, but calculation is also possible from knowledge of product composition together with the resulting quantity of energy absorbed by the products in comparison with that released by the reactants (Borman and Ragland 1998). The maximum temperature is reached, of course, when all the reaction energy is released and then absorbed by the products, with no transfer of work or heat to the environment. This product temperature is high (in order of 2000 K), and therefore, the products are not in simple mixtures of gases as suggested by simple atom balances to determine stoichiometric coefficients. Rather, the major species dissociate, producing a host of minor species. For example, the ideal combustion products for burning a hydrocarbon with air are CO_2 , H_2O , O_2 , N_2 , H_2 and CO . Dissociation of these yield OH , H , O and possibly others, in endothermic reactions.

In nature, one of the spontaneous tendencies is towards minimum energy, but a second natural tendency is to the increasing entropy. Consequently, when fuels and oxidants are reacting spontaneously, the driving forces are directed towards a reduction in their total stock of energy, denoted by enthalpy, and an increase in their overall disorder, denoted by entropy. Using thermodynamic analysis it can be shown that at equilibrium condition, Gibbs energy, ($G \equiv H - TS$) is minimized. Thus, at equilibrium condition:

$$(\Delta G)_{P,T} \leq 0 \quad (2.25)$$

For a given general reaction (Eqn. 2.8), the value of ΔG is given by

$$\Delta G_T = \sum_{prod} \nu_j g_j - \sum_{react} \nu_i g_i \quad (2.26)$$

The sign of ΔG_T is important since a negative value indicates that the given reaction is feasible. Gibbs energy change, ΔG_T , is related to the chemical equilibrium coefficient, K_p , (Turns 2000):

$$K_p = \exp \left[-\frac{\Delta G_T}{R_u T} \right] \quad (2.27)$$

Equation 2.27 gives an qualitative indication of whether a particular reaction favors products (goes strongly to completion) or reactants (very little reaction occurs) at equilibrium. If ΔG_T is positive, reactants will be favored and vice versa. Physical insight to this behavior can be obtained by the application of the definition of ΔG in terms of enthalpy and entropy change associated with the reaction. Hence, Equilibrium coefficient, K_p can be written as:

$$K_p = \exp \left(-\frac{\Delta H_T}{R_u T} \right) \cdot \exp \left(\frac{\Delta S_T}{R_u} \right) \quad (2.28)$$

For equilibrium constant, K_p , to be greater than unity, which favors products, the enthalpy change for the reaction, ΔH_T , should be negative, i.e. the reaction is *exothermic* and the system energy is lowered. Hence, more the reaction is exothermic more it will favor the products and vice versa. Also, endothermic reactions will be slower for all other conditions remaining the same. Moreover, positive change in entropy, which indicate greater molecular chaos, lead to values of $K_p > 1$. It is not surprising that, K_p is not a function of total pressure of the system, rather a function of temperature alone (Glassman 1996). However, the effect of pressure on the product composition is observed when K_p is expressed in terms of mole-fractions and pressure. The relationship is given by Heywood (1988) as:

$$K_p = \frac{\prod [P]^{\nu_j}}{\prod [R]^{\nu_i}} \left[\frac{P}{P_{ref}} \right]^{(\sum \nu_j - \sum \nu_i)} \quad (2.29)$$

Depending of the values of stoichiometric coefficients, three cases are possible:

1. $(\sum \nu_j - \sum \nu_i) = 0$: changes in pressure have no effect on the compositions.
2. $(\sum \nu_j - \sum \nu_i) > 0$: these are dissociation reactions. Hence, the mole fractions of the dissociation products are decreased as pressure increases.
3. $(\sum \nu_j - \sum \nu_i) < 0$: these are recombination reactions. Hence, reaction is favored with increase in pressure.

These observations are in accordance with Le Châtelier principle.

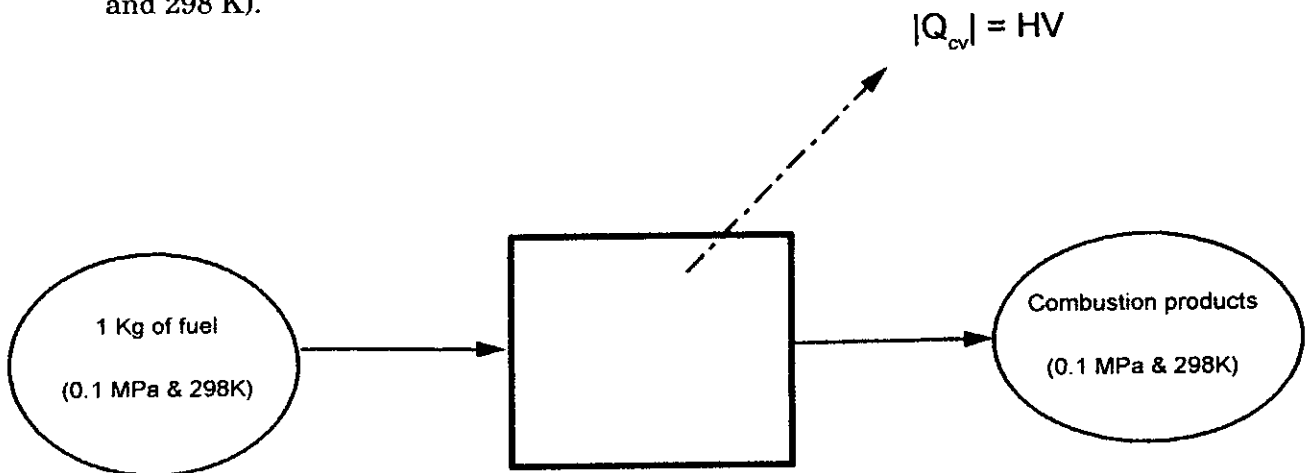
If all the heat evolved in the complete combustion reaction is employed solely to raise the product temperature, the resulting temperature is called adiabatic flame temperature and the product composition is known as equilibrium composition. Therefore, reactant mixture enthalpy, $H_{react}(T_i, P)$, is same as the product enthalpy, $H_{prod}(T_{ad}, P)$. Hence,

$$H_{react}(T_i, P) = H_{prod}(T_{ad}, P) \quad (2.30)$$

Both of these enthalpies are estimated using thermodynamic principles (§ 2.3). Adiabatic flame temperature, T_{ad} , is an intrinsic property of any combustible mixture and is estimated through some iteration procedure to satisfy enthalpy conservation law (Eqn. 2.30) by estimating equilibrium compositions at that estimated temperatures (§ 2.3), and continued iteration until Eqn. 2.30 satisfied within specified accuracy.

2.6 Estimation of Heat Release

Heat release during combustion can be estimated using energy balance. A schematic is shown below for the combustion of 1 Kg of fuel with stoichiometric amount of air under standard conditions of pressure and temperature (0.1 MPa and 298 K).



Enthalpy of reaction (or combustion) (Δh_R), can be estimated using:

$$\Delta h_R = h_{prod} - h_{react} \quad (\text{kJ/kg-fuel}) \quad (2.31)$$

Hence, the values of h_{react} and h_{prod} are estimated using principles (§ 2.3) with prior knowledge of product composition at low temperature of 298 K. Lower heating value is a more practical value than HHV, and is used in estimating the specific energy, $SE_{\phi\beta}$, and energy density, $ED_{\phi\beta}$. Values of these quantities are estimated using the following relationships:

$$LHV = |h_{prod} - h_{react}| \quad (\text{kJ/kg-fuel}) \quad (2.32)$$

$$SE_{\phi\beta} = |h_{prod} - h_{react}| Y_{fuel} \quad (\text{kJ/kg-mix}) \quad (2.33)$$

$$ED_{\phi\beta} = SE_{\phi\beta} \rho_{mix} \quad (\text{kJ/m}^3\text{-mix}) \quad (2.34)$$

where, Y_{fuel} is the mass fraction fuel in charge, and ρ_{mix} is the density of charge. It may also be noted that, the values of h_{prod} are not same in Eqns. 2.32 and 2.33. To estimate heating values, complete combustion stoichiometric mixture is used. For heat release from off-stoichiometric charge, additional species are to be included depending on the stoichiometric condition of initial premixture.

2.7 Estimation of Chemical Equilibrium Composition

Although in any combustion process, major reactions are at temperatures near to the adiabatic flame temperature. However, some reactions are slow and are generally termed as 'post flame reaction's. These reactions are not completed as a result of heat transfer in the exhaust manifold. Hence, product composition is modified depending on heat transfer, available time and exhaust temperature and results in different composition. Combustion equilibrium combustion products at low temperatures are important because of ever increasing concern over the environmental problems, and this composition is also required to estimate the amount of heat release as explained in § 2.6.

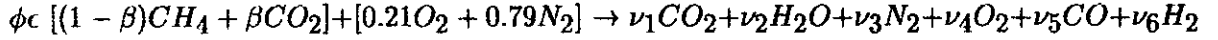
Several methods are available to estimate adiabatic flame temperature and equilibrium compositions.

- Newhall and Starkman chart (Ferguson 1960)
- Equilibrium temperature chart (Glassman 1996).
- Using equilibrium rate constant, K , correlations of Olikara and Bowman (1975)
- Minimizing Gibbs energy (Lutz and Rupley 1994).

There are several commercial/share-ware programs capable of estimating equilibrium compositions at adiabatic flame temperatures. However, there is no suitable code available to estimate of low temperature product composition for methane and bio-gas combustion. The product compositions are estimated using spreadsheet with some practical assumptions.

2.7.1 Estimation of Product Composition at Low Temperature

Combustion reaction for bio-gas air mixture of equivalence ratio, ϕ , can be written as:

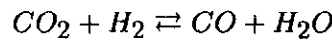


In practical combustion, product mixture contain a large number of other species in very small amount and these quantities are often neglected. For non-stoichiometric charge combustion, the product mixture is assumed to contain CO , O_2 and H_2 , in addition to the stoichiometric combustion products. The stoichiometric coefficients of the product mixtures are estimated using atom balance and thermodynamic principles. Conventional approximations for the lean and rich conditions are:

$$\phi \leq 1 : \nu_5 = \nu_6 = 0 \quad (2.35)$$

$$\phi > 1 : \nu_4 = 0 \quad (2.36)$$

For lean or stoichiometric conditions, atom balance equations are sufficient to determine the product composition (four equations and four unknowns). For the rich conditions, it is necessary to introduce the *Water Gas Shift Reaction*:



This reaction accounts for the simultaneous presence of incomplete combustion products, CO and H_2 , in addition to the complete combustion products, CO_2 and H_2O . This is a pressure independent equation and equilibrium constant, K_p , is given by the following relationship:

$$K_p = \frac{\nu_2 \nu_5}{\nu_1 \nu_6} = \frac{[0.42 - 2\phi\epsilon(1 - \beta) + \nu_5][\nu_5]}{[\phi\epsilon - \nu_5][4\phi\epsilon(1 - \beta) - 0.042 - \nu_5]} \quad (2.37)$$

Hence, K_p is estimated for the water gas shift reaction to provide the additional equation to solve the problem for rich conditions. Solution of low temperature combustion, in moles per mole of air, are given in Table 2.2.

Table 2.2. Low temperature combustion products, ν_j (moles/mole of air)

	$\phi \leq 1$	$\phi > 1$
CO_2	$\phi\epsilon$	$\phi\epsilon - \nu_5$
H_2O	$2\phi\epsilon(1 - \beta)$	$0.42 - 2\phi\epsilon(1 - \beta) - \nu_5$
N_2	0.79	0.79
O_2	$0.21 - 2\phi\epsilon(1 - \beta)$	0
CO	0	ν_5
H_2	0	$4\phi\epsilon(1 - \beta) - 0.42 - \nu_5$

2.7.2 Estimation of T_{ad} and Product Compositions

For high temperature combustion, simple atom balances and use of water gas shift reaction is not sufficient. At high temperatures, simultaneous presence of enormous amount of product species makes the solution very difficult. Fortunately, several code are available that are capable of predicting accurate combustion product composition and adiabatic temperatures using detailed reaction mechanism. In the present study, Sadia equilibrium code, EQUIL (Lutz and Rupley 1994), is used. To estimate the equilibrium composition and temperature, it is required to provide, in a keyword format, the initial pressure, temperature, reactant mole fractions and an guess of adiabatic temperature to start with the iteration. A typical output from EQUIL code is reported in Appendix. A.

2.8 Results and Discussion

Shown in Fig 2.1 are the heating values of methane and bio-gas with different percentages of CO_2 , expressed by β . It is observed that higher heating values are always higher than lower heating values, however the discrepancy decreases with increase β . This is because of the formation of lesser amount of water for a given amount of fuel. It is also observed that increasing β results in decrease of heating values, as amount of CO_2 present in bio-gas do not have any heating value, rather it absorbs heat from the combustion products. The values of HHV and LHV of iso-octane is also marked in Fig. 2.1.

Shown in Fig. 2.2(a) are the variation of specific energy, $SE_{\phi\beta}$, as a function of equivalence ratio, ϕ , for various percentages of CO_2 . Values of energy density, $ED_{\phi\beta}$ are plotted in Fig. 2.2(b) for the similar conditions as in Fig. 2.2(a). It is observed that the heat release for a given amount of charge (mass or volume) depend on both ϕ and β . Heat releases decrease with increasing β in line with the findings of heating values shown in Fig. 2.1. It is also observed that the heat releases are maximum for stoichiometric mixture, and their values decrease as ϕ deviates from stoichiometric conditions. It is also observed that heat release for rich mixture are higher than at lean mixtures. This is due to the fact that, although rich mixture contain more fuel to burn, there is less amount of oxygen to complete the combustion process and this combustion product contains species that are capable of further oxidation and heat release.

Estimation of heating values requires the estimation of equilibrium composition at 298K where reactions have different pathway as compare to that one for at high temperatures. A brief review of possible alternative reaction pathways are presented in Appendix B. For high temperature combustion, water gas shift reaction is very significant. Shown in Fig. 2.3(a) are the product mole fractions of CO and CO_2 for different ϕ , at temperatures of 298 K, 500 K, 1000 K and T_{ad} . Hence, CO concentration, $[CO]$, is practically negligible while $[CO_2]$ increases nearly linearly with ϕ , at $T = 298$ K. However, with increase in temperature results in the

increases of $[CO]$, with associated decrease in $[CO_2]$. Shown in Fig. 2.3(b) are variations of $[H_2]$ and $[H_2O]$ for different ϕ , at temperatures of 298 K, 500 K, 1000 K and T_{ad} . It is seen that, $[H_2O]$ increases nearly linear with ϕ for lean mixtures without significant temperature effects, while it reaches a maximum at stoichiometric conditions and then decreases with ϕ . However, this decrease is higher at lower temperatures. It is also seen that, $[H_2]$ is practically negligible for lean mixtures and linearly increases with ϕ for rich mixtures. However, this increase is higher at lower temperatures. Shown in Fig. 2.3(c) are the variations of $[O_2]$ and $[N_2]$ as a function of ϕ . Values of $[O_2]$ are practically negligible for rich mixture where insufficient amount of oxygen is present in the process; and excess O_2 present with lean mixtures remain with the product. It is also seen that the values of $[O_2]$ and $[N_2]$ are practically unaffected by the temperature change.

Shown in Fig. 2.4 are the dissociation reaction of $[CO_2]$, $[H_2]$ and $[O_2]$ at initial pressures of 0.1 and 1.0 MPa as a function of temperatures. It is seen that all the three cases, dissociation is suppressed by increase in pressure which in line with Le Châtelier principle (§ 2.5). Dissociation is also found to increase with increase in temperature. However, below 2000 K, dissociation of H_2 and O_2 are practically negligible, while the CO_2 is considerable at 1500 K. In practical cases, these dissociation are often neglected where flame temperatures are lower than 1500 K.

Shown in Fig. 2.5 are the adiabatic flame temperature, T_{ad} 's, and mole fractions of major combustion products and some minor products plotted as a function of ϕ . In Fig. 2.5(a), lower flammability limit (LFL) and higher flammability limit (HFL) of methane-air mixture are also marked, these values embrace the flammability zone beyond which no flame propagation is possible (Turns 2000). It is seen that, maximum flame temperature is not at stoichiometric, rather, at slightly rich condition ($\phi \approx 1.05$). This maximum temperature is at a slightly rich condition is a consequence of lower mean specific heats of richer products (Glassman 1996). Lower mean specific heats of richer product is owing to the preponderance of the diatomic molecules CO and H_2 in comparison to the triatomic molecules CO_2 and

H_2O . The diatomic molecules have lower molar specific heats than the triatomic molecules. For a given enthalpy content of reactants, the lower the mean specific heat of product mixture, the greater the final flame temperature.

Flame temperatures deviate from the maximum value with the deviation of ϕ . However, flame temperature at HFL is higher than at LFL. This is not surprising because of the lower specific heat capacities of the richer mixtures in addition to more available energies, as shown in Fig. 2.2. It is seen in Fig. 2.5(b) that, the major products of lean combustion are H_2O , CO_2 , O_2 and N_2 (N_2 is not shown as it is a major product at all conditions of ϕ); and for rich combustion the major products are H_2O , CO_2 , CO , H_2 and N_2 . At stoichiometric conditions O_2 , CO and H_2 are present, whereas for the assumption of complete combustion, i.e., no dissociation, these three species should be zero. Minor species of equilibrium combustion products at the flame temperature include O , H and OH , as shown in Fig. 2.5(c). Carbon monoxide is a minor species in lean products, while O_2 is a minor species in rich products. It is also noted that the concentrations of minor species H , O and OH are practically negligible when compared with the major species, although the concentration of OH is much higher than that of H and O .

Shown in Fig. 2.6 are the variation of T_{ad} as a function of ϕ for different values of β at initial pressures of 0.1 and 1.0 MPa. The effect of pressure is found negligible for off-stoichiometric conditions. Increase in pressure suppresses dissociation, and dissociation is found important, only at near stoichiometric conditions. Dissociation are endothermic reactions and therefore suppression of it results in higher temperatures. Flame temperature decreases with increase in β as a result of lower energy contents, as shown in Fig. 2.2.

Densities of product mixture follows the ideal gas law, which is shown in Fig. 2.7. For increase in β results in increase in density. This is due to fact that CO_2 is heavier than other combustion products. It is interesting to note that, minimum density results at slightly richer conditions as a result of the combined effects of resulting flame temperature and CO_2 composition.

Shown in Fig. 2.8 are the variations of $[O_2]$ as a function of ϕ , for different values of β at initial pressures of 0.1 and 1.0 MPa. The effect of pressure on O_2 concentration is found negligible, while O_2 concentration decreases slightly with increase in β . Hence, the CO_2 acts as inserts only to decrease the resultant concentrations of O_2

Shown in Fig. 2.9 are the variations of $[CO_2]$ as a function of ϕ for different values of β at initial pressures of 0.1 and 1.0 MPa. The effect of pressure on $[CO_2]$ is found negligible only at off-stoichiometric conditions. At near stoichiometric conditions, flame temperature is high enough to cause dissociation of CO_2 to CO . At pressure suppresses dissociation and it results in a higher $[CO_2]$ at near stoichiometric conditions. It is also seen that, values of $[CO_2]$ of increase with β .

Shown in Fig. 2.10 are the variations of concentration of CO as a function of ϕ , for different values of β at initial pressures of 0.1 and 1.0 MPa. The effect of pressure on CO concentration is found negligible. Concentration of CO is practically negligible for lean mixtures while its concentration increases with ϕ and β at rich conditions. The increase in CO concentration with β results from water gas shift equation (§ 2.7.1).

The importance of water gas shift reaction is found to be very significant in establishing equilibria between CO , CO_2 , H_2 and H_2O . It is seen that, any increase in the CO_2 concentration results in increase in $[CO]$ and $[H_2O]$ and also causes decrease in $[H_2]$. This effect is shown in Fig. 2.10 for the variation of $[CO]$, while values of $[H_2]$ and $[H_2O]$ are shown Figs. 2.11 and 2.12, respectively. It is also important to note that, this reaction is not effected by pressure. The negligible pressure effect on these concentration are also seen in these figures.

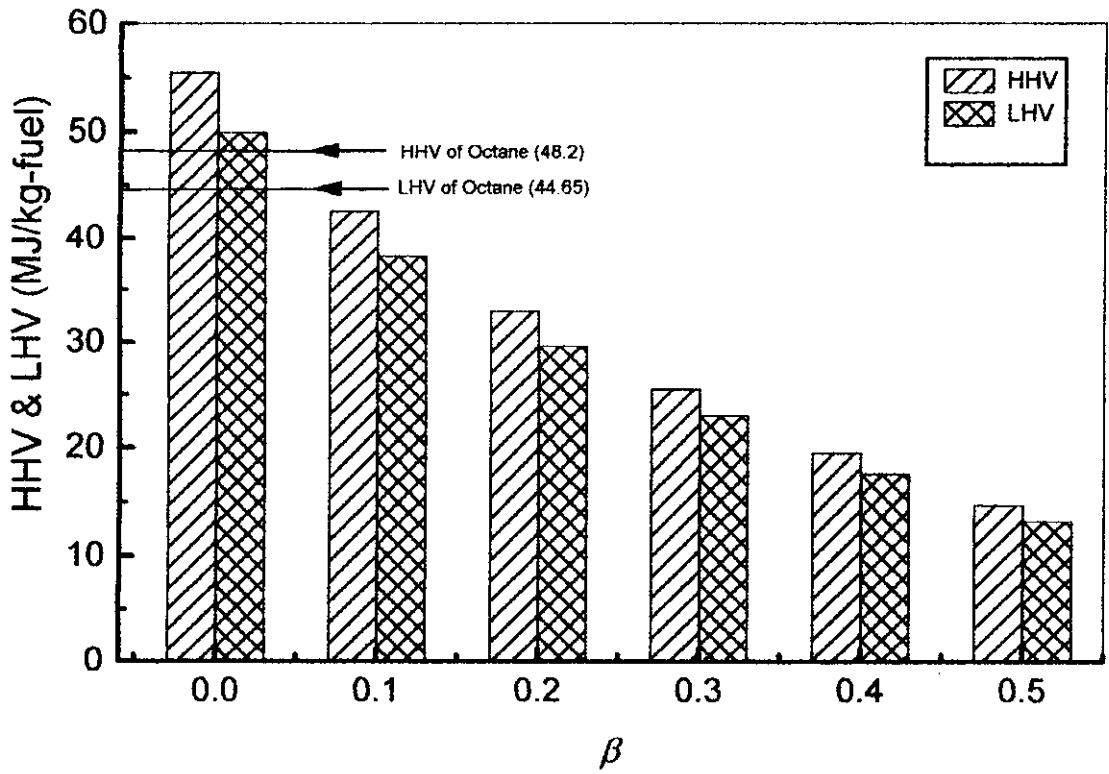


Fig. 2.1. Heating values for a bio-gas at different values of β .

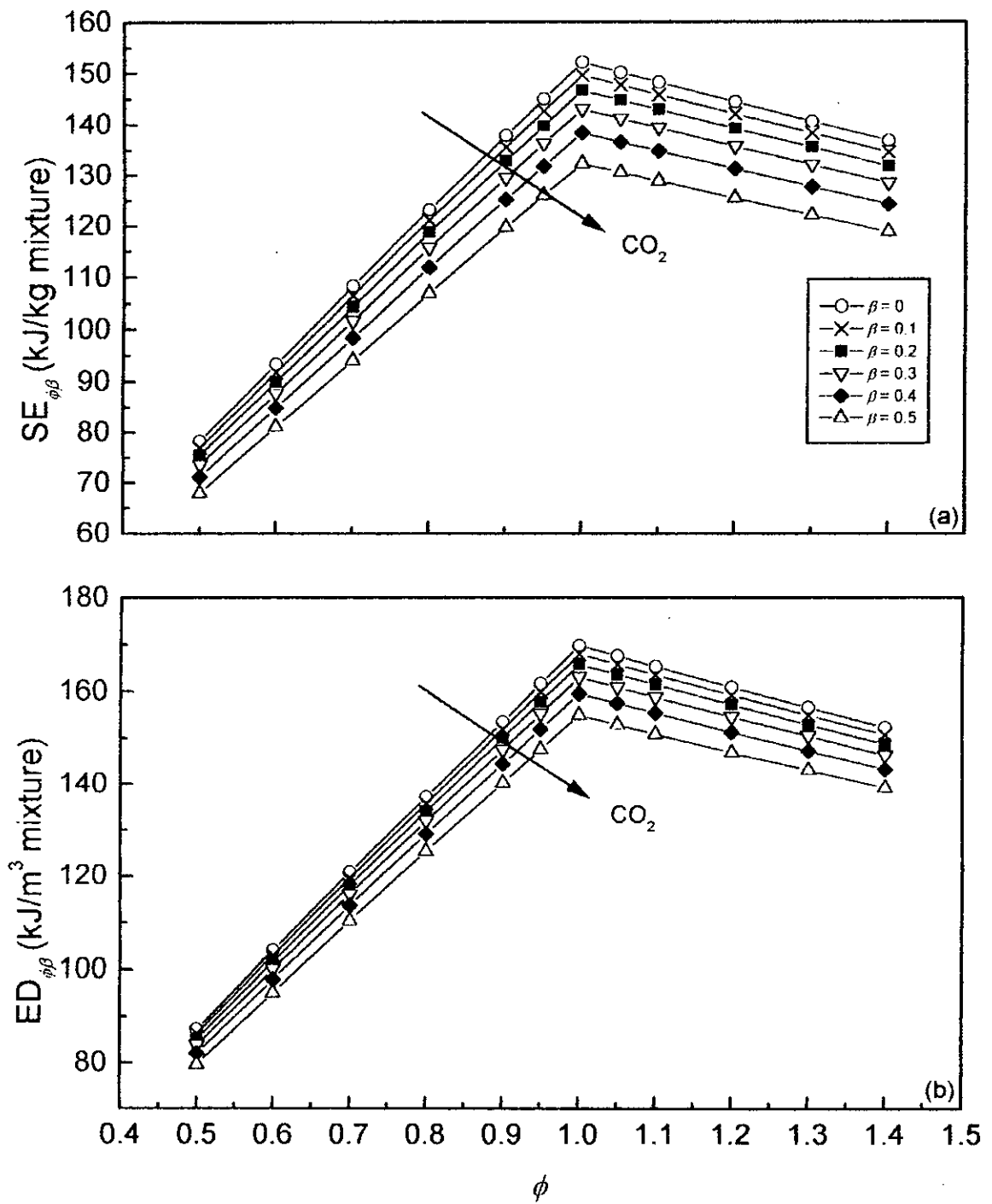


Fig. 2.2. Specific Energy and Energy Density for bio-gas air premixture as a function of ϕ .

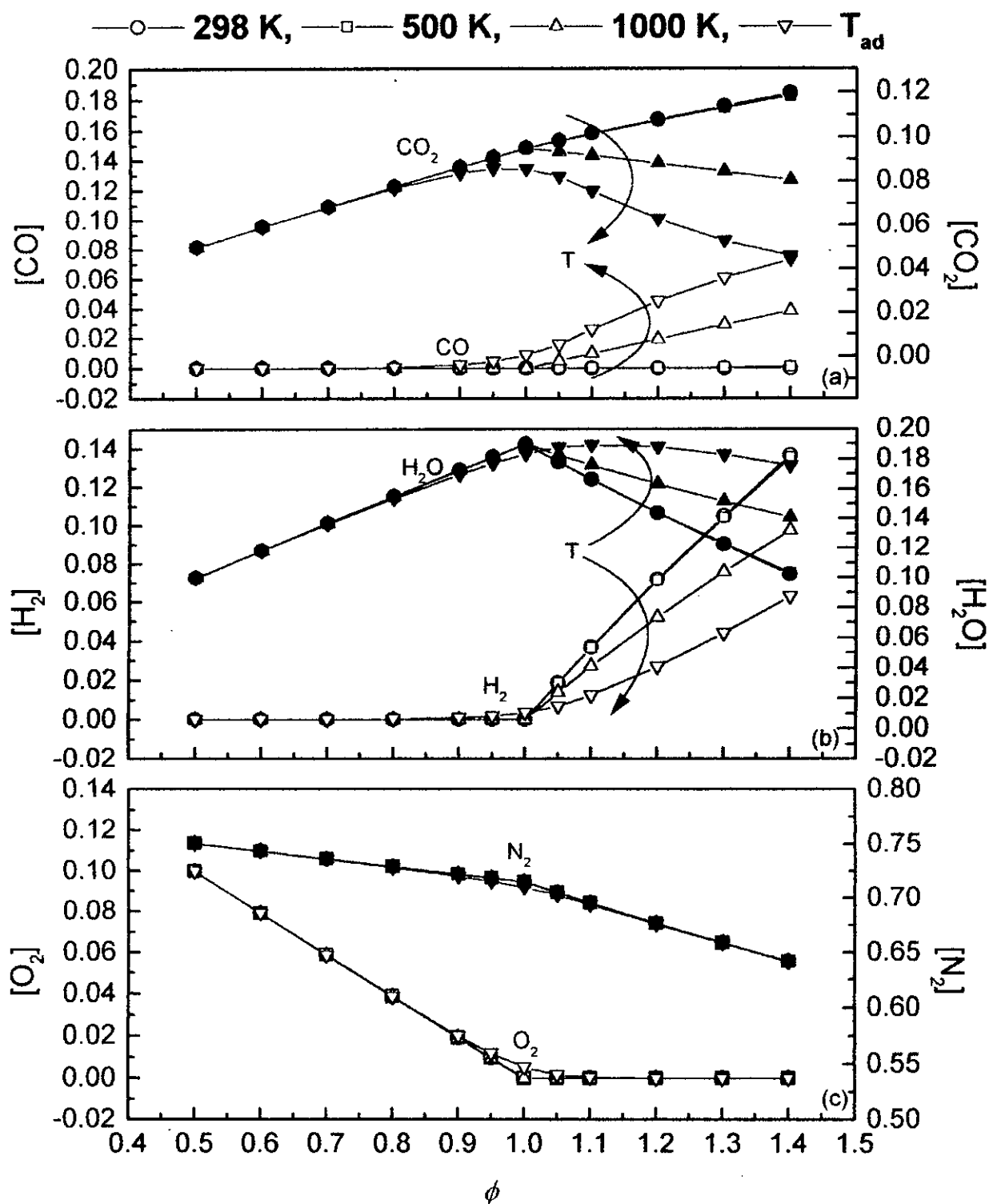


Fig. 2.3. Combustion product equilibrium composition of $[CO_2]$, $[CO]$, $[H_2O]$, $[H_2]$, $[N_2]$ and $[O_2]$ as a function of ϕ at different temperature.

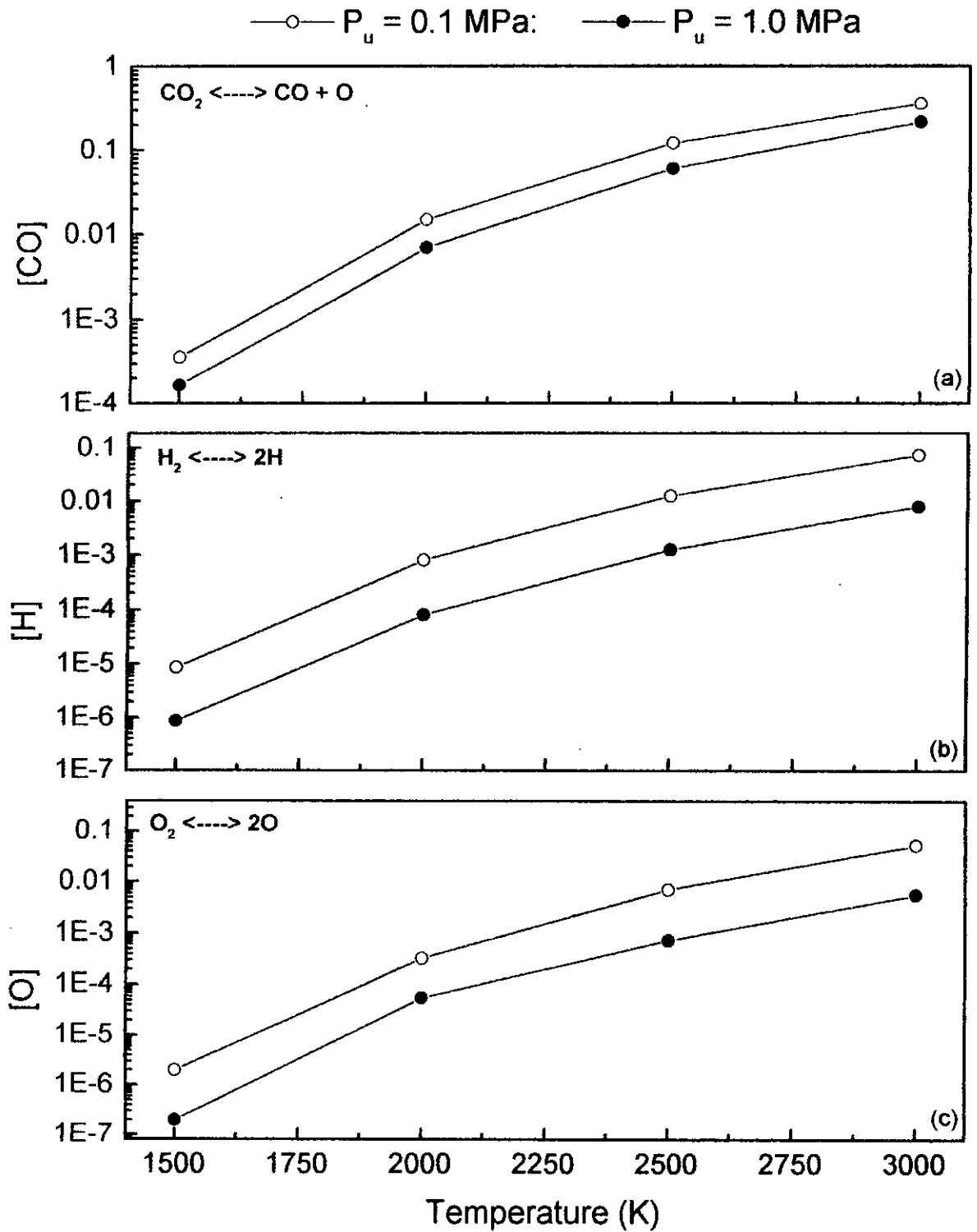


Fig. 2.4. Dissociation of CO_2 , H_2 and O_2 as a function of temperature.

27
CH₄-air Mixture at 0.1 MPa

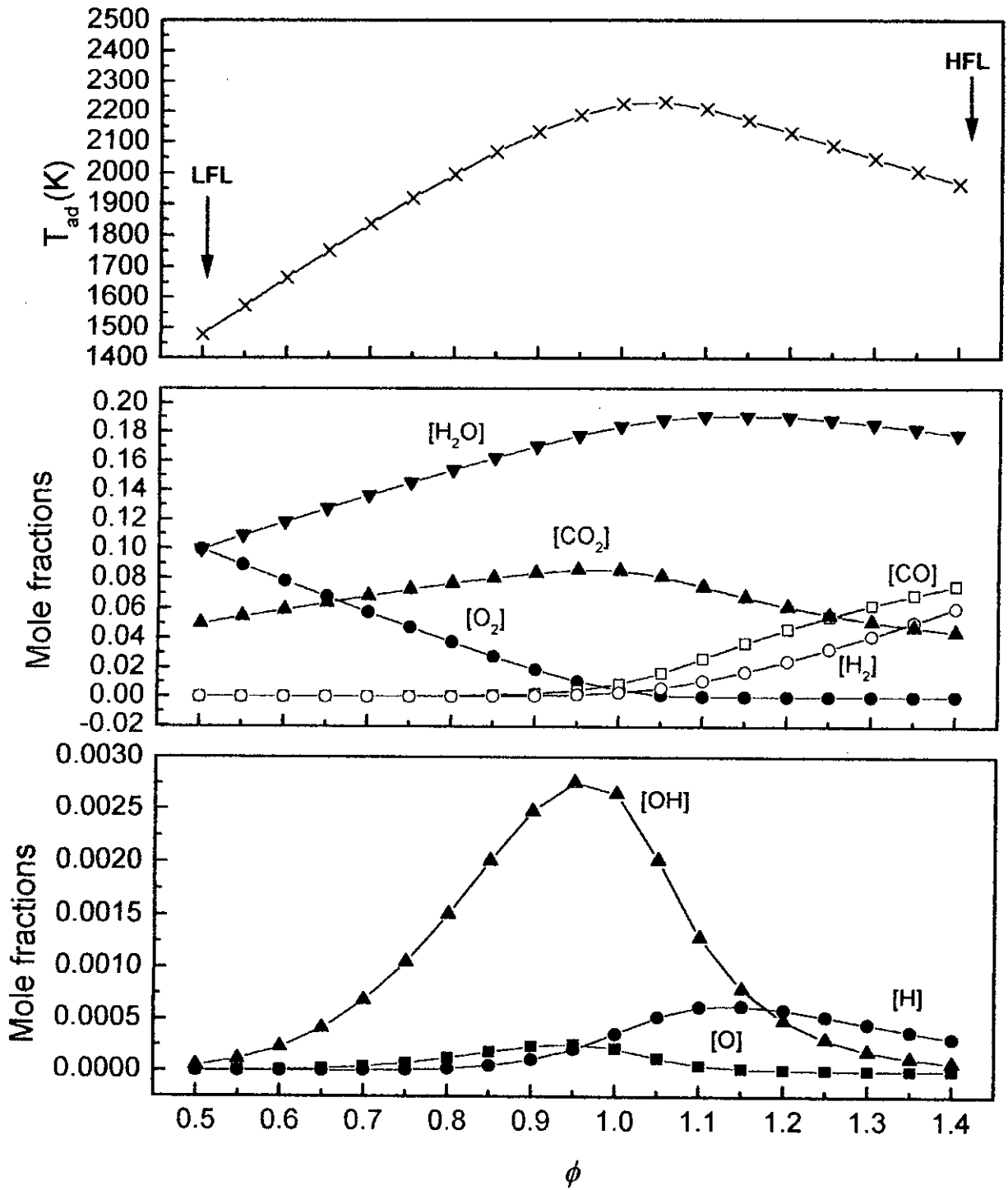


Fig. 2.5. Mole fractions of equilibrium combustion products and adiabatic temperatures of methane-air premixture as a function of ϕ .

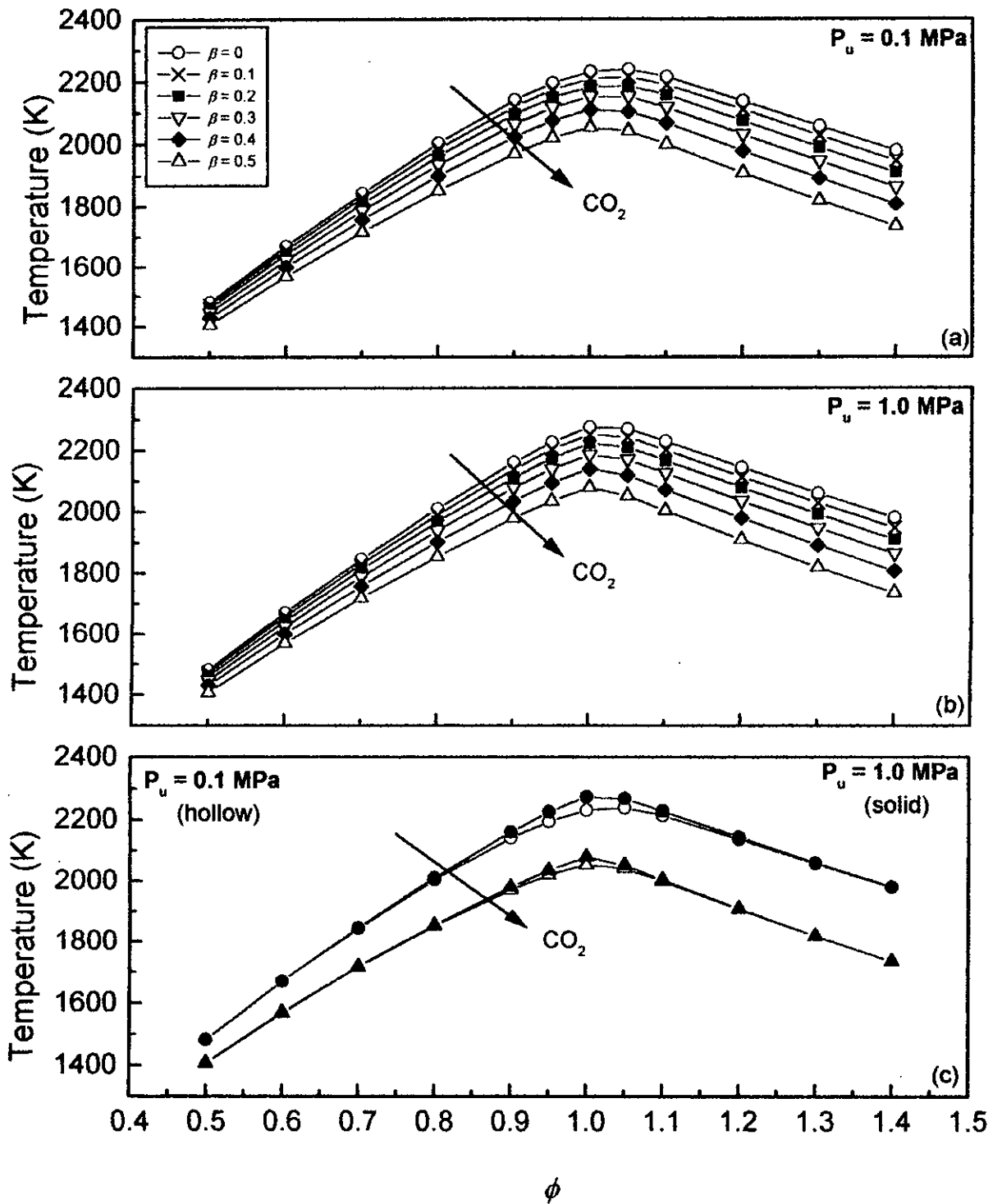


Fig. 2.6. Variation of T_{ad} 's as a function of ϕ for different values of β at two initial pressures of 0.1 and 1.0 MPa.

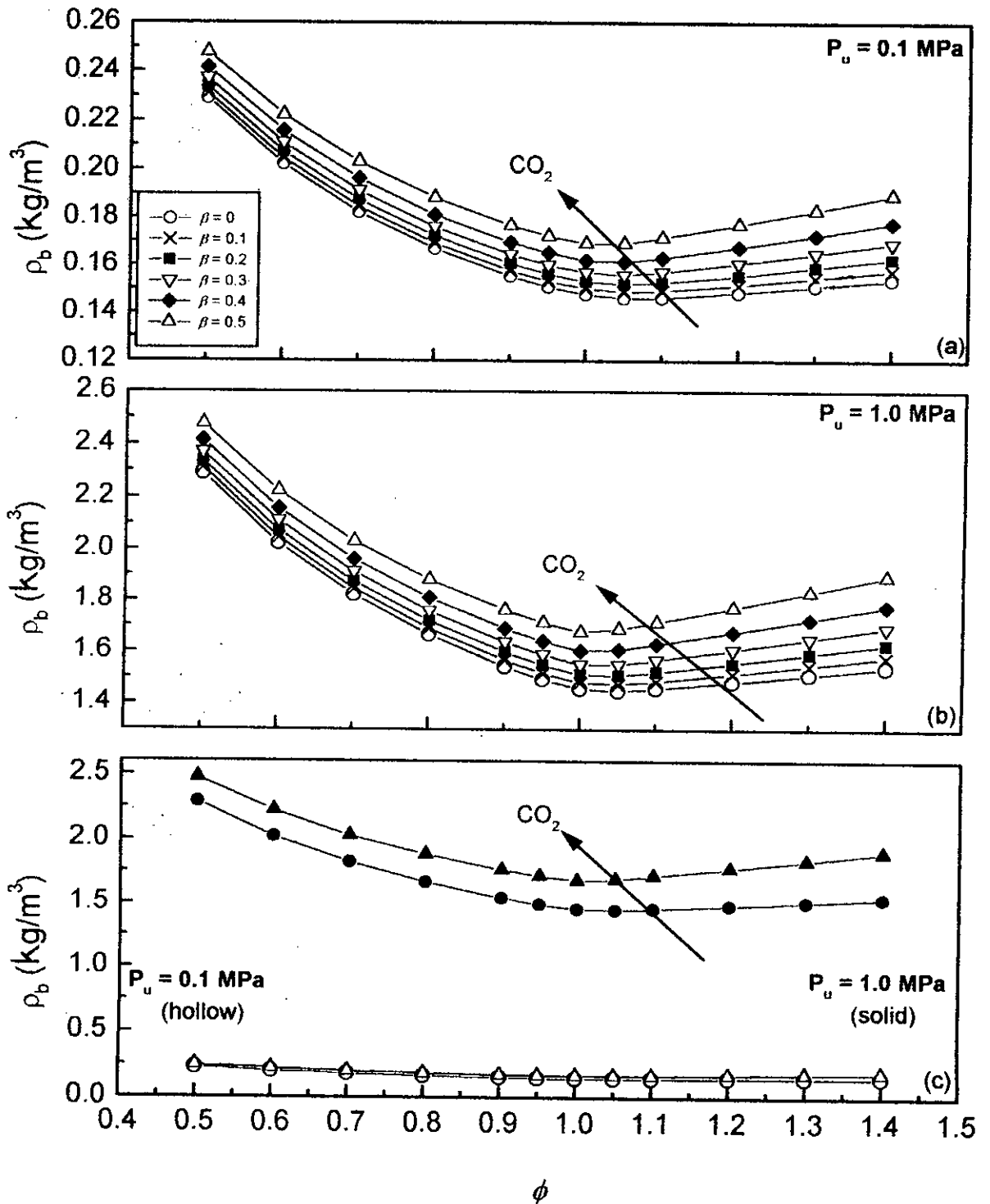


Fig. 2.7. Variation of ρ_b 's as a function of ϕ for different values of β at two initial pressures of 0.1 and 1.0 MPa.

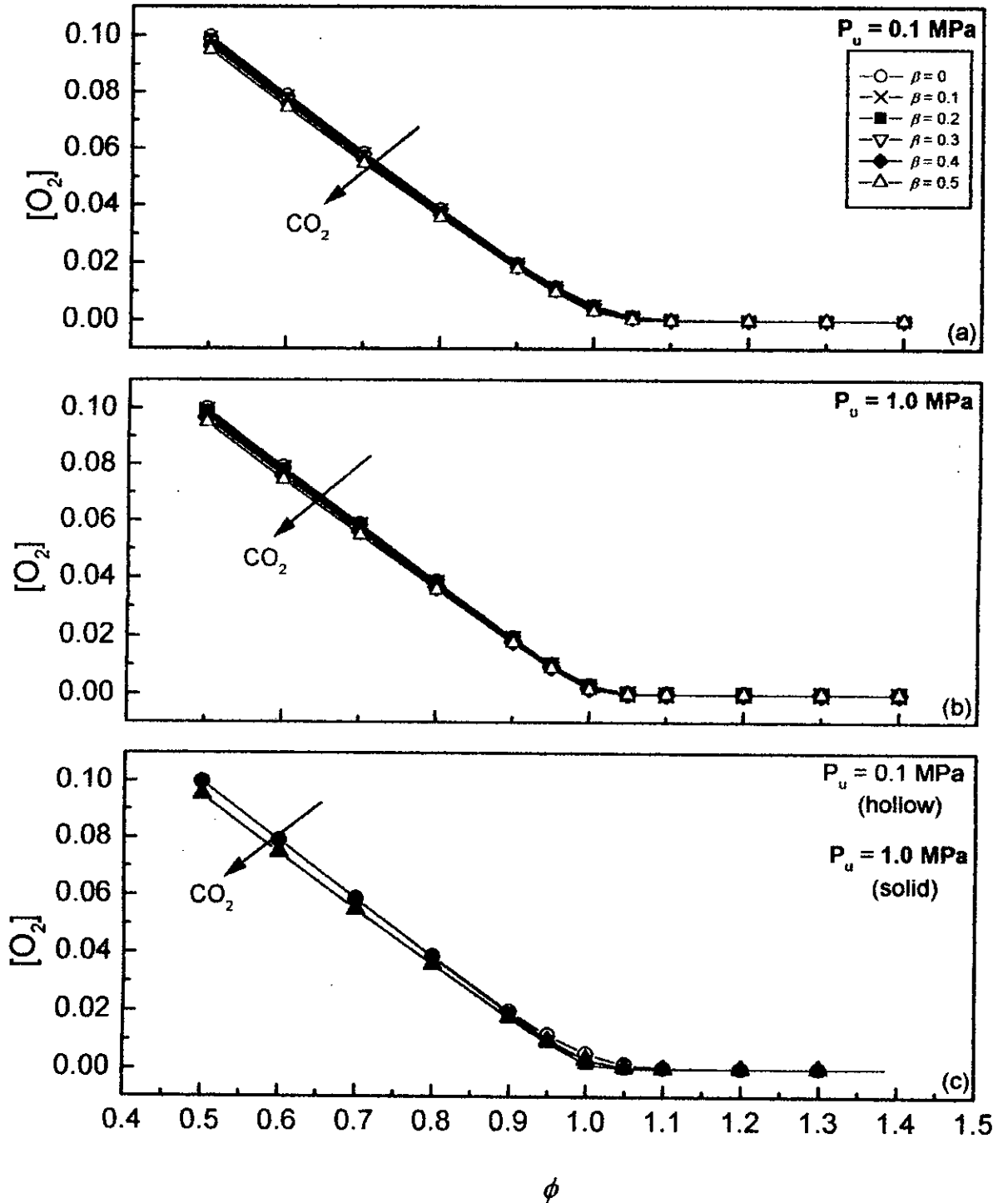


Fig. 2.8. Variation of $[O_2]$'s as a function of ϕ for different values of β at two initial pressures of 0.1 and 1.0 MPa.

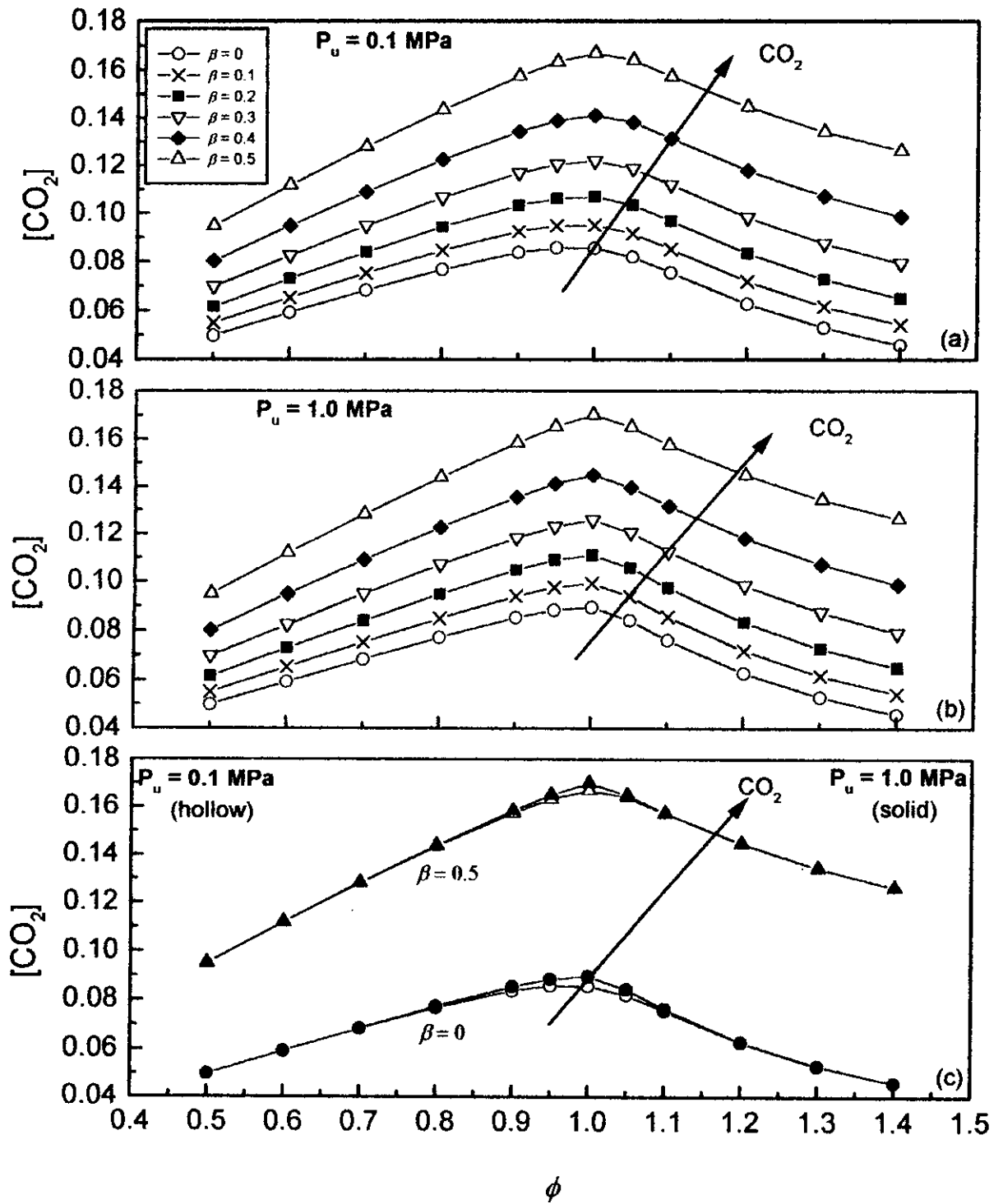


Fig. 2.9. Variation of $[CO_2]$'s as a function of ϕ for different values of β at two initial pressures of 0.1 and 1.0 MPa.

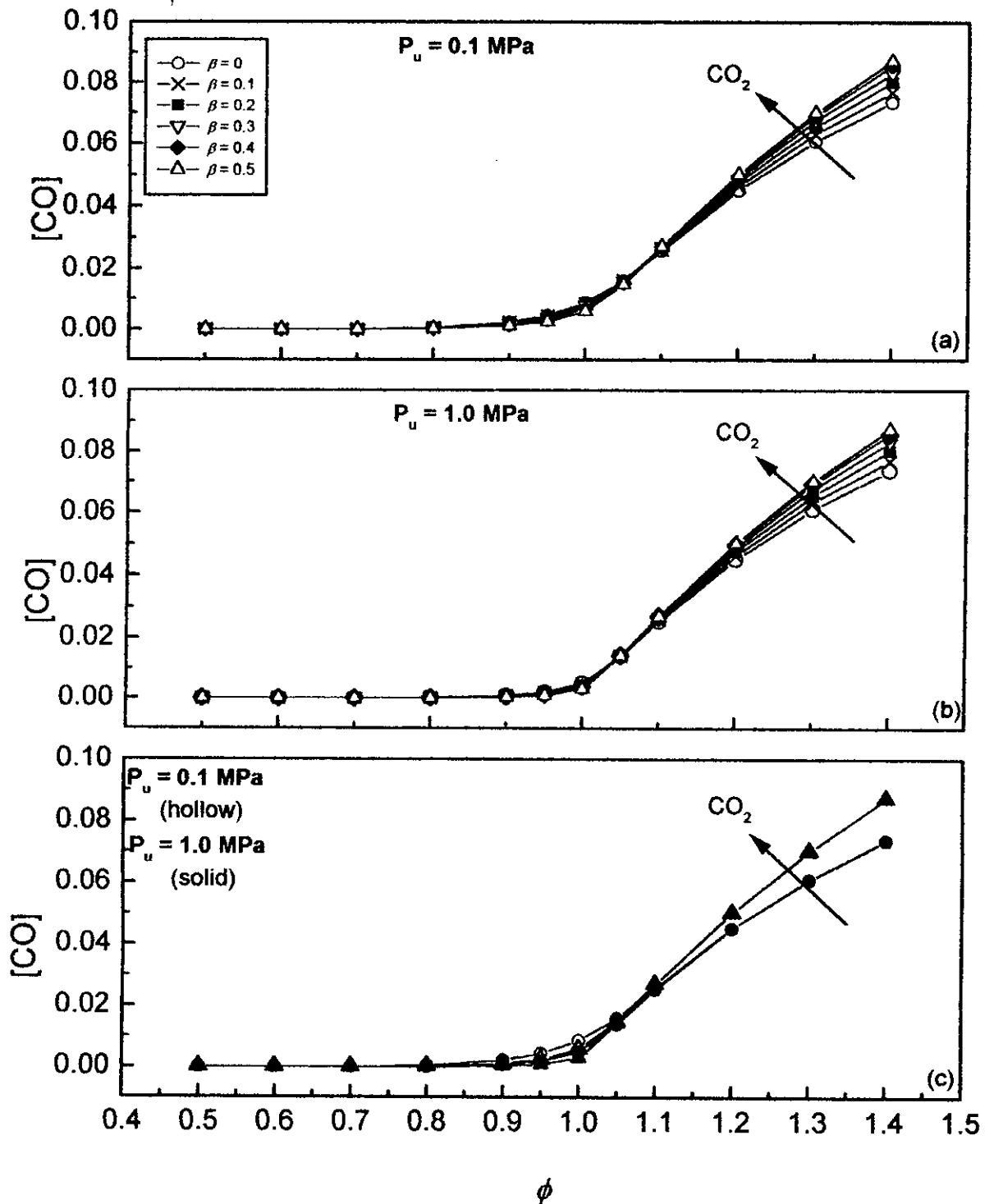


Fig. 2.10. Variation of $[CO]$'s as a function of ϕ for different values of β at two initial pressures of 0.1 and 1.0 MPa.

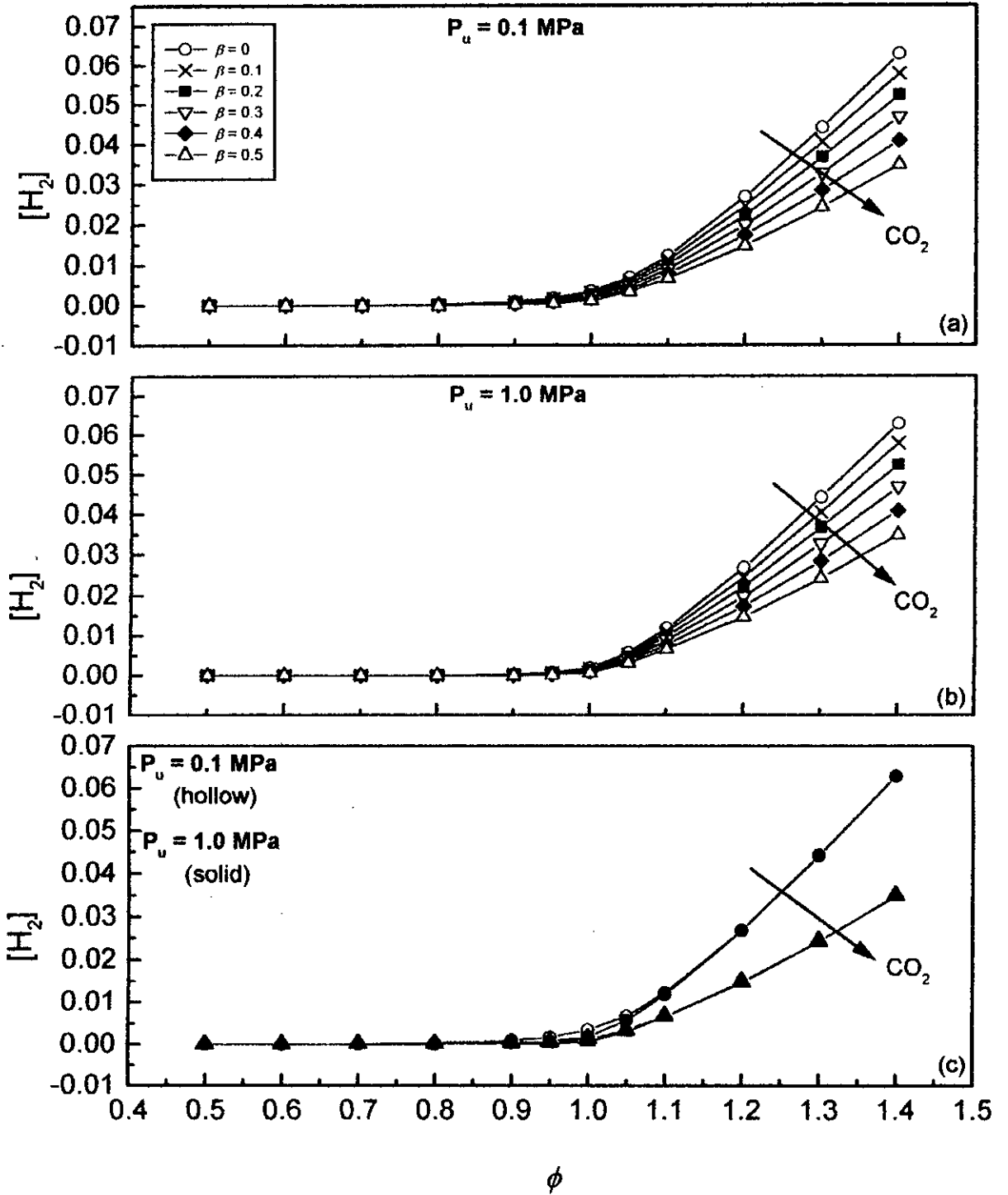


Fig. 2.11. Variation of $[H_2]$'s as a function of ϕ for different values of β at two initial pressures of 0.1 and 1.0 MPa.

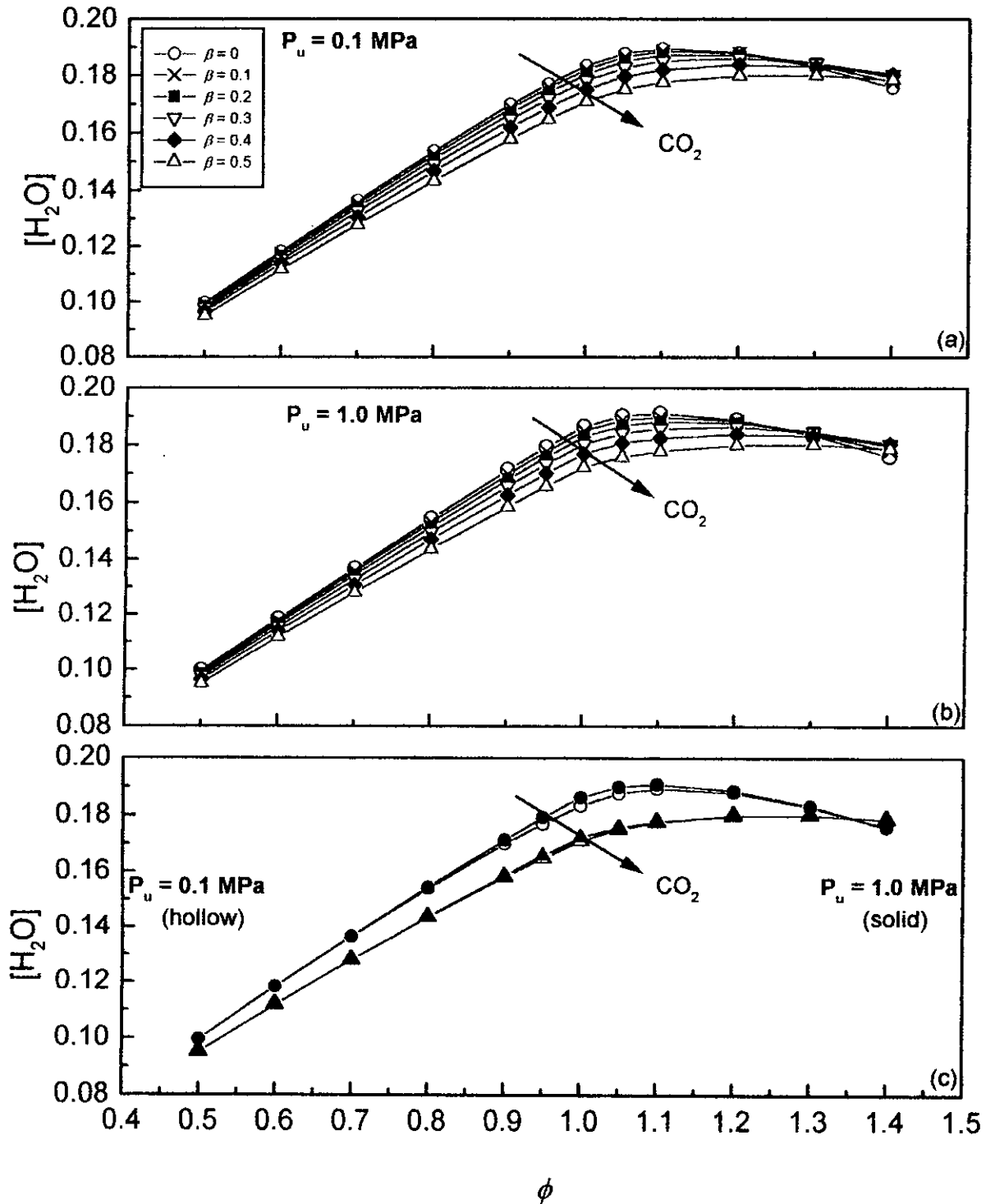


Fig. 2.12. Variation of $[H_2O]$'s as a function of ϕ for different values of β at two initial pressures of 0.1 and 1.0 MPa.

Chapter 3

Bio-gas Air Flame Structure and Laminar Burning Velocities

The structure and propagation of laminar premixed flame are governed by convection, diffusion and chemical reactions that are frequently characterized by large activation energies and high heat release rates. Early studied on flames have pursued along two directions, either assuming the flame structure simple or keeping the flame chemistry and transport processes simple (Law and Sung 2000). Structure of the adiabatic, one-dimensional, freely propagating planar premixed flames at increasingly detailed level of description is reported in (Law and Sung 2000) (Shown in Fig. 3.1). With the tremendous advances in both computing power and techniques, it is now possible to model detailed analysis of laminar flame structure and burning velocities. Hence, Laminar burning velocity, u_f , is an intrinsic property of a combustible fuel-air mixture, and is defined as 'the velocity, relative to and normal to the flame front, with which the unburned gas moves into the front and is transformed into products under laminar flow conditions' (Heywood 1988).

In the present study, one-dimensional adiabatic flame propagation in laminar bio-gas air premixture is modeled with detailed chemistry and transport processes. Laminar burning velocities at different compositions are studied at two initial pressures of 0.1 and 1.0 MPa, at 300 K.

3.1 Modeling of Premixed Adiabatic Laminar Flame

Theories of laminar flames have occupied many researchers for many decades. For example, Turns (2000) cited more than a dozen of major papers dealing with laminar flame theory. Most of these analyses bear the essential physics and chemistry without a great deal of mathematics because of the constrained computational capabilities. To determine the laminar burning velocity and to study the detailed flame structure, it is now possible to solve by computational techniques the governing equations of one-dimensional, steady, planar, adiabatic, isobaric premixed flames. These governing equations are:

Overall Continuity:

$$\dot{m} \equiv \rho u = \text{constant} \quad (3.1)$$

Species Conservation:

$$\dot{m} \frac{dY_i}{dx} + \frac{d}{dx}(\rho Y_i v_{i,\text{diff}}) = \dot{\omega}_i M_i \quad (3.2)$$

Energy Conservation:

$$\dot{m} c_p \frac{dT}{dx} + \frac{d}{dx} \left(-k \frac{dT}{dx} \right) + \sum \rho Y_i v_{i,\text{diff}} C_{p,i} \frac{dT}{dx} = - \sum h_i \dot{\omega}_i M_i \quad (3.3)$$

It may be noted that, momentum equations are not considered in subsonic premixed flame analysis because of isobaric flame propagation (Strehlow 1984). In addition to these conservation equations, the following ancillary relations or data are required:

Ideal Gas Equation of State: It provides the basic relationship among pressure, P , temperature, T and density, ρ , of ideal gas species or mixture § 2.1.

Constitutive Relationship for Diffusion Velocities: For general problem of species diffusion in multicomponent mixtures, total diffusion velocity, $v_{i,\text{diff}}$, of species, i

is given by Turns (2000) as:

$$v_{i,\text{diff}} = v_{i,\text{diff},X} + v_{i,\text{diff},T} + v_{i,\text{diff},P} + v_{i,\text{diff},f} \quad (3.4)$$

where, subscripts X , T , P and f , refer to ordinary, thermal, pressure and force diffusion, respectively. In typical combustion process, diffusion due to pressure and force are usually neglected leaving only two diffusion components, namely diffusion due to concentration gradient (ordinary) and due to temperature (Glassman 1996).

Ordinary diffusion, $v_{i,\text{diff},X}$, depends in a very complex way on both the mixture composition, through the appearance of the component mole fractions, X_i , and on the individual binary diffusion coefficients for pairs of species, D_{ij} (Kuo 1986). Hence, ordinary diffusion velocity is given by Turns (2000) as:

$$v_{i,\text{diff},X} = -\frac{D_{im}}{X_i} \frac{dX_i}{dx} = -\left[\frac{1 - X_i}{\sum_{i \neq j} X_j / D_{ij}} \right] \frac{1}{X_i} \frac{dX_i}{dx} \quad (3.5)$$

Values of D_{ij} are estimated using kinetic theory of gases and review of these are available in literature (Bird, Stewart, and Lightfoot 1960; Kuo 1986; Turns 2000).

Thermal diffusion velocity, $v_{i,\text{diff},T}$ is rather simple and is given by Turns (2000) as:

$$v_{i,\text{diff},T} = -\frac{\alpha_{mix}}{X_i} \frac{1}{T} \frac{dT}{dx} \quad (3.6)$$

where, the thermal diffusivity of mixture, α_{mix} and is given by:

$$\alpha_{mix} = \frac{k_{mix}}{\rho u C_{p,mix}} \quad (3.7)$$

hence, the thermal conductivity of the mixture, k_{mix} is calculated using the semi-empirical formula of Mason and Saxena (1958) from thermal conductivity of gases species components. Thermal conductivity of pure gaseous species are estimated using kinetic theory of gases and details are available in literature (Bird, Stewart, and Lightfoot 1960; Kuo 1986; Turns 2000).

Thermodynamic Properties: Temperature dependent species properties $h_i(T)$, $C_{p,i}(T)$ are estimated using NASA type polynomials as discussed in § 2.1.

Detailed Chemical Kinetic Mechanism: The net chemical production rate, $\dot{\omega}_i$, of each species, i , results from a competition between all the chemical reactions involving that species. It is usually presumed that each elementary reaction proceeds according to *the law of mass action* and the forward rate coefficients, k_f , are expressed, in general, in the modified Arrhenius form as (Turns 2000):

$$k_f = AT^b \exp\left(-\frac{E_A}{R_u T}\right) \quad (3.8)$$

hence, A , b , E_A are the empirical parameters. In the present study, GRI-Mech 1.2 (Frenklach *et al.* 1995) is used to describe methane and bio-gas air combustion in terms of 177 elementary step reactions of 32 species. In GRI-Mech 1.2, values of A , b , E_A are provided for all 177 elementary step reactions in addition to the reactions itself. These reactions are not simple consecutive steps, rather they offer several alternative parallel and consecutive pathways for reactions to proceed, depending on the initial conditions of pressure, temperature and composition. A very brief introduction of this alternative pathway analysis of low and high temperatures are presented in Appendix B, and the reaction mechanism is presented in Appendix C.

Boundary Conditions: The conservation relations describe a boundary value problem; i.e. given information about the unknown function (T, X_i) at an upstream location (boundary) and a downstream location (boundary).

The problem at hand is to determine the function $T(x)$ and $X_i(x)$ between these boundaries. Hence, the boundary conditions are:

$$T(x \rightarrow -\infty) = T_u \qquad Y_i(x \rightarrow -\infty) = X_{i,0} \qquad (3.9)$$

$$\frac{dT}{dx}(x \rightarrow +\infty) = 0 \qquad \frac{dY_i}{dx}(x \rightarrow +\infty) = 0 \qquad (3.10)$$

Moreover, an additional boundary condition is required, or alternatively one degree of freedom must be removed from the problem. In PREMIX code (Kee *et al.* 1985) flame is assumed to be anchored at a given temperature, T_{fix} , by specifying the temperature at one point in the flame domain. This is sufficient to allow for the solution of the mass flux eigenvalue, \dot{m} . Temperature, T_{fix} is selected in such a way as to insure that the temperature and species gradients "nearly" vanish at the cold boundary to eliminate the so called problem *cold boundary difficulty* (Law 1984). If this condition is not met then the resultant \dot{m} will be too low because some heat will be lost through the cold boundary.

3.2 Computation Technique and Program Structure

In the present study, unstrained laminar burning velocity and flame structure of a freely propagating, one-dimensional, adiabatic premixed flame are computed using the Sandia PREMIX code (Kee *et al.* 1985). This uses a hybrid time integration/Newton Iteration technique to solve the steady state, comprehensive mass, species and energy conservation equations. Hence, the mass flux, \dot{m} , is not known prior but is an eigen value of the problem - its value is a part of the solution, and since the unburned gas mixture density is readily known, the laminar burning velocity, u_l , is estimated.

PREMIX flame code is written in two major modules. One is a piece of software to solve boundary value problems; it is completely independent and could easily be used for problems not related to flames. The other module contains the

flame specific coding. It reads input from the user, defines the governing equations, makes calls to the boundary value solver, and prints solutions for the flame problem.

In addition to input directly from the user, the flame program depends on data and subroutines from the CHEMKIN (Kee *et al.* 1989) and transport package, TRAFIT (Kee *et al.* 1986). Therefore, to solve a flame problem, it is required to set up a command procedure that allows for the execution of several preprocessor programs, the access to several data-bases, the loading of subroutines from several libraries, and the passing of files from one process to another. Shown in Fig. 3.2 is the basic relationships between these various components.

The first step is to execute the CHEMKIN interpreter (Kee *et al.* 1989). It interpreter first reads (Unit 5) user-supplied information about the species and chemical reactions for a particular reaction mechanism. It then extracts further information about the species' thermodynamic properties from a data base (Unit 21). This information is stored on the CHEMKIN linking file (Unit 25); a file that is needed by the transport property fitting program, TRANFIT, and later by the CHEMKIN subroutine library, which will be accessed by the flame program. In addition, the CHEMKIN interpreter requires an additional binary scratch file on Unit 23.

The next program to be executed is the transport property fitting program, TRANFIT (Kee *et al.* 1986). It needs input from a transport property data base (Unit 31) and from the CHEMKIN subroutine library. Its purpose is to compute polynomial representations of the temperature-dependent parts of the individual species viscosities, thermal conductivities, and the binary diffusion coefficients. Like the CHEMKIN interpreter, the TRANFIT program produces a linking file (Unit 35) that later needed in the transport property subroutine library, which will evaluate mixture properties during the course of the flame computation.

Both the CHEMKIN and transport subroutine libraries must be initialized before use and the flame program makes the appropriate initialization calls. The

purpose of the initialization is to read the linking files and set up the internal working and storage space required by all subroutines in the libraries.

The input that defines a particular flame and the parameters needed to solve it are read by PREMIX in a keyword format from Unit 5. In addition, there is a provision for the flame program to begin its iteration from a previously computed flame solution. In this case the old solution is read from a restart file assigned to Unit 14. The flame program produces printed output on Unit 6 and it saves the solution on Unit 15. The saved file can be used either to restart the same problem and continue iterating, or it can be read as a starting estimate for a different flame, which, for example may have different unburned species compositions or flow rates.

3.3 Problem Solution, Convergency and Consistency of Solution

To solve combustion problem at a given initial condition of P , T and ϕ , it is required to provide the following major input data, in a keyword format from unit 5 (§ 3.4):

- Pressure, P , Temperature, T , and initial mole fraction, X_i , of reactant species,
- Size of computational domain and estimated position of flame,
- Number of initial grid points to start with and maximum total grid number,
- Estimate of $T(x)$ at different locations within the computational domain.
- Absolute and relative tolerances for the termination of calculation iteration.
- Estimate of major combustion products, X_j ,
- Estimate of intermediate species concentration,

An example input data file is reported in Appendix D, for modeling of stoichiometric methane-air mixture at in initial conditions of 300 K and 0.1 MPa.

Using PREMIX code, solution is made as initial grid points which is usually small to meet the specified accuracy. Subsequently, more grid points are inserted at locations where temperature and species profiles vary considerably. Shown in Fig. 3.3 is such an example where laminar burning velocity, u_l , is plotted as a function of number of grid points. It is seen that, beyond certain number of grid points, the values of u_l 's are changed asymptotically and an increasing in number of grid points do not contribute significantly to its values; however, any increase in number of grid points costs more computer time. Hence, refinement of grid points are continued until solution meets the specified accuracy and then the solution is assumed to be converged.

The results obtained form PREMIX code are also verified against the results obtained using 'RUN-1DL: The laminar flame and flamelet code' (Rogg and Wang 1997). Shown in Fig. 3.4 is an example of such a comparison, where symbols represent the values obtained using RUN-1DL, while solid line represents the results obtained using PREMIX. Close agreement between these results from these two different codes and techniques emphasizes the importance of studying laminar flame structure numerically to provide detailed insight into the flame structure.

3.4 Results and Discussions

Shown in Fig. 3.5(a) is the variation of flame temperature as a function of axial distance for stoichiometric methane-air flame at 0.1 MPa and 300 K, while the mole fractions of major species are shown in Fig 3.5(b). Adiabatic flame temperature, T_{ad} and ignition temperature, T_{ig} are also marked in the Fig. 3.5(a). Ignition temperature is the temperature where flame reaction really turns on producing heat. It is seen that the temperature increases rapidly after this temperature and approaches T_{ad} , only in asymptotic manner. The axial distance, corresponding to the segment of the tangent spanning the interval between T_u and T_{ad} , is termed as *flame thickness*. In the zone, denoted by the flame thickness is the zone where most of the chemical activities occur. Upstream of this *reaction zone* is the *preheat*

zone and the downstream is the *post flame reaction zone*. In Fig. 3.5(b), the disappearance of fuel and O_2 , and the appearance of CO , CO_2 , H_2O and H_2 are clearly visible. It is seen that $[CO]$ has its peak value at approximately the same location where the $[CH_4]$ goes to zero, while the CO_2 at first lags $[CO]$, but then continues to rise as the $[CO]$ is oxidized. Note also that, H_2O reaches its 80% of equilibrium mole fraction much sooner than does the CO_2 . While the fuel is completely gone in approximately 1 mm and the major portion of the total temperature rise (73%) occurs in the same interval, the approach to equilibrium conditions is relatively slow beyond this point. In fact, we see that equilibrium has yet to be reached even at the 2.5 mm location. However, all these concentrations approaches their adiabatic equilibrium compositions in an asymptotic manner.

Shown in Fig. 3.6 are variation of flame temperatures, plotted against axial distance. In Fig. 3.6(a), flame temperature profiles for different ϕ are shown, while in Fig. 3.6(b) the effects of pressure and β are shown. It is seen that flame is thick for off-stoichiometric conditions, its value decrease with increase in pressure. However, with increase in β , flame becomes thicker. All of the temperature profiles approaches their corresponding T_{ad} 's.

Shown in Fig. 3.7 are variation of $[CH_4]$, plotted against axial distance. In Fig. 3.7(a), $[CH_4]$ profiles for different ϕ are shown, while in Fig. 3.7(b) the effects of pressure and β are shown. This flame thickness variations here are clearly visible by the disappearance of $[CH_4]$. It is seen that flame is thick for off-stoichiometric conditions, its value decrease with increase in pressure. However, with increase in β , flame becomes thicker. All of the temperature profiles approaches their corresponding equilibrium compositions. However, it is interesting to note that, for even very rich conditions $\phi = 1.4$, no CH_4 is found in the downstream of the flame.

Shown in Fig. 3.8 are variation of $[O_2]$, plotted against axial distance. In Fig. 3.8(a), $[O_2]$ profiles for different ϕ are shown, while in Fig. 3.8(b) the effects of pressure and β are shown. This flame thickness variations here are clearly visible by the disappearance of $[O_2]$, as observed for $[CH_4]$ in Fig. 3.7. It is also noted

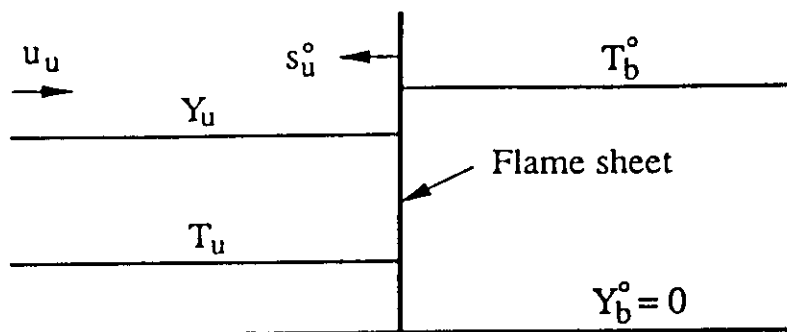
that, for lean conditions, O_2 is present. At stoichiometric conditions $[O_2]$ is not zero, because of the dissociation. For rich condition, O_2 is practically negligible.

The similar effect of composition and pressure on flame thickness are also seen, in a opposite manner to Fig. 3.7 and Fig. 3.8, by the appearance of burned products, H_2O and CO_2 , respectively, in Figs. 3.9 and 3.10. However, slower oxidation of CO is also clearly visible in Fig. 3.10.

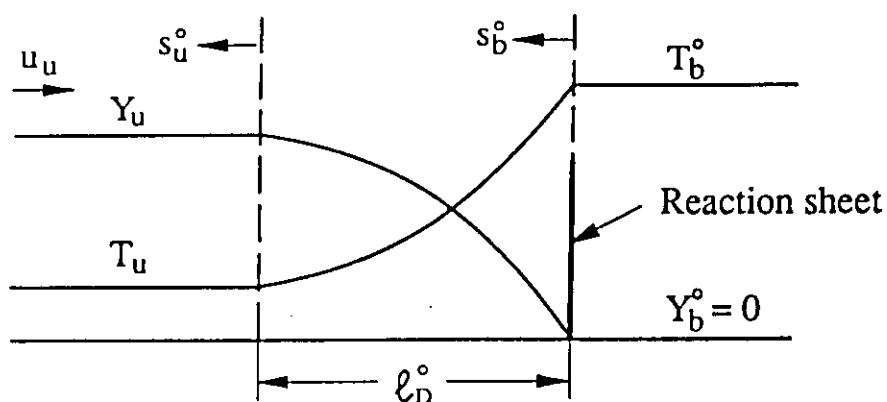
Shown in Figs. 3.11 and 3.12 are the values of $[CO]$ and $[H_2]$, respectively, for different initial conditions of pressure and composition. For lean conditions, their concentration is very small. Their values have their peaks at the flame reaction zone, and they are after-burned to reach their equilibrium values further in the downstream.

Shown in Fig. 13 are the mass flux, \dot{m} , values for different initial conditions of pressure and composition. For off-stoichiometric combustion, its value is lower than the stoichiometric values and any increase in pressure results in higher flux. However, mass flux reduces with increases with β because of slower combustion.

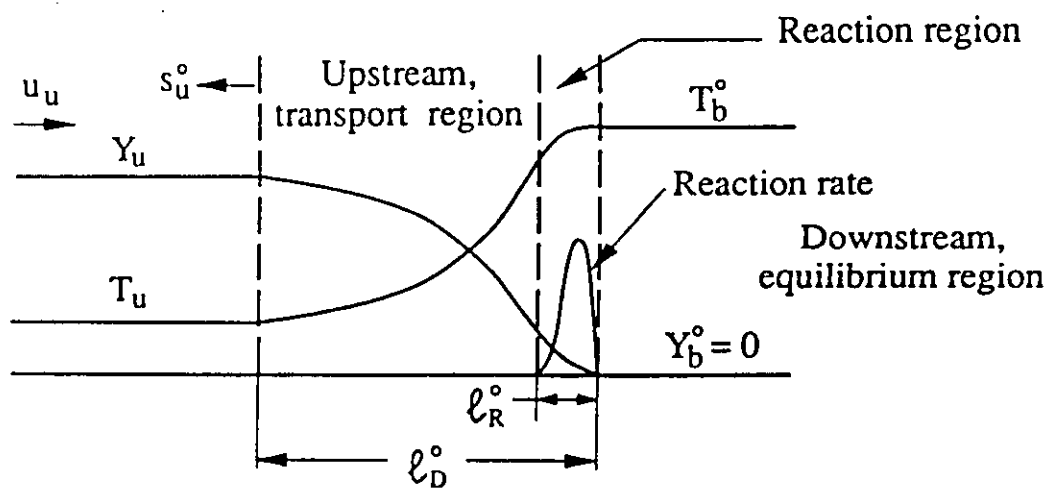
From the values of mass flux, \dot{m} , it is possible to estimate the corresponding laminar burning velocity, u_l , as shown in Fig. 3.14. Burning velocities reaches its maximum value, not surprising at $\phi = 1.05$, where T_{ad} is also maximum. It emphasizes the effect of T_{ad} on the laminar burning velocities. Any increase in β , results in a lower T_{ad} and hence, lower u_l . The effect of β is similar in high pressure, as shown in Fig. 3.14(b). However, high pressure flames are always slow, as found in the experimental studies of Gu *et al.* (2000). This reduction is attributed to different chemistry at higher pressures.



(a)



(b)



(c)

Fig. 3.1. Structure of the adiabatic, one-dimensional, freely propagating planar premixed flame at increasingly detailed levels of description: (a) hydrodynamic level; (b) transport level; and (c) reaction level.

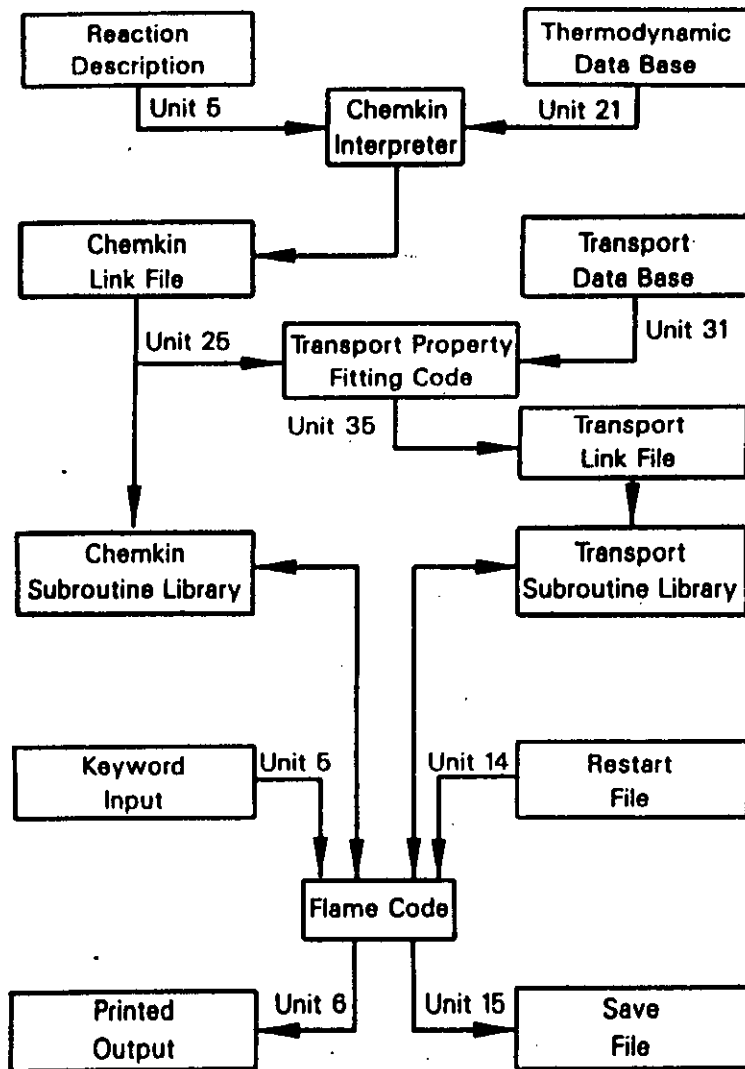


Fig. 3.2. Relationship of PREMIX to CHEMKIN and TRANFIT; and the associated input and output files.

Methane-air mixture
 $P_u = 0.1 \text{ MPa} \ \& \ \phi = 1.0$

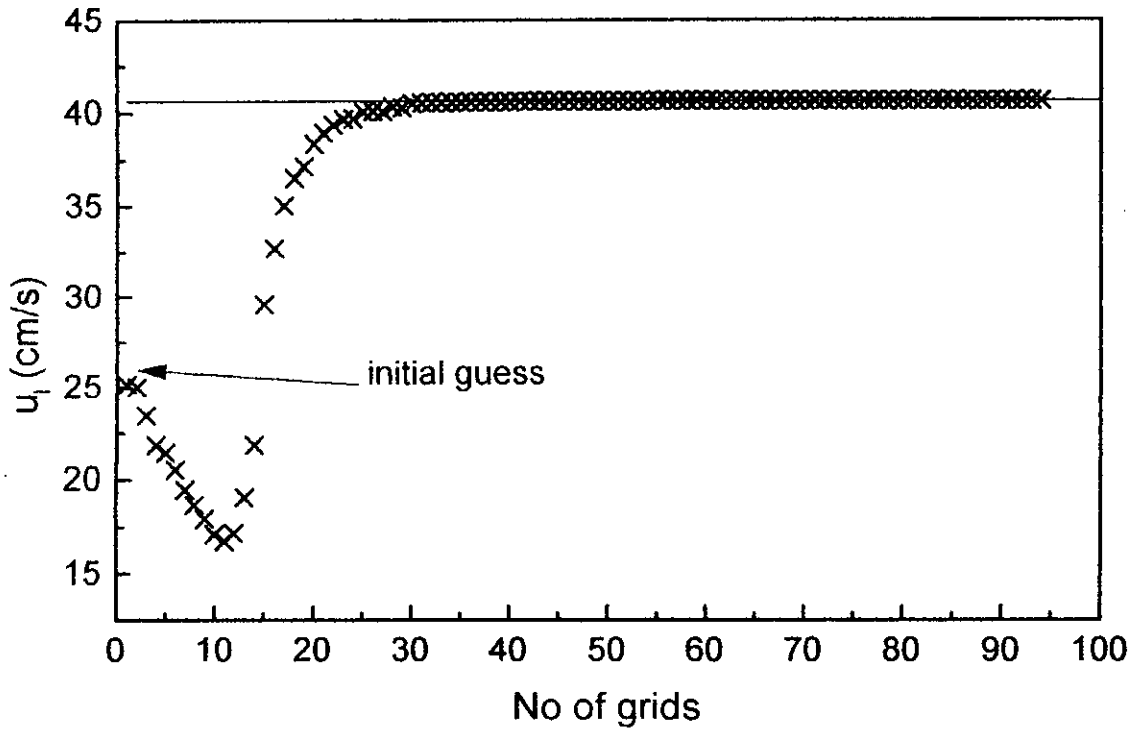


Fig. 3.3. Test of convergence of solution using PREMIX.

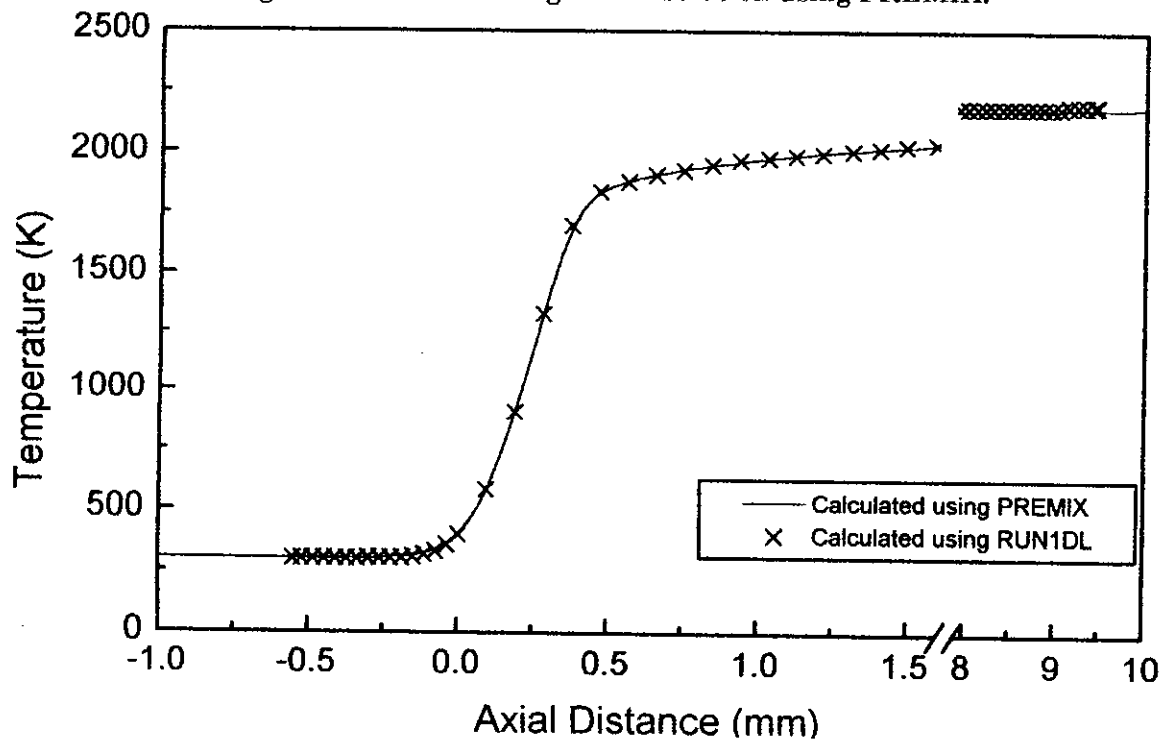


Fig. 3.4. Example of comparison of results of PREMIX with RUN-1DL.

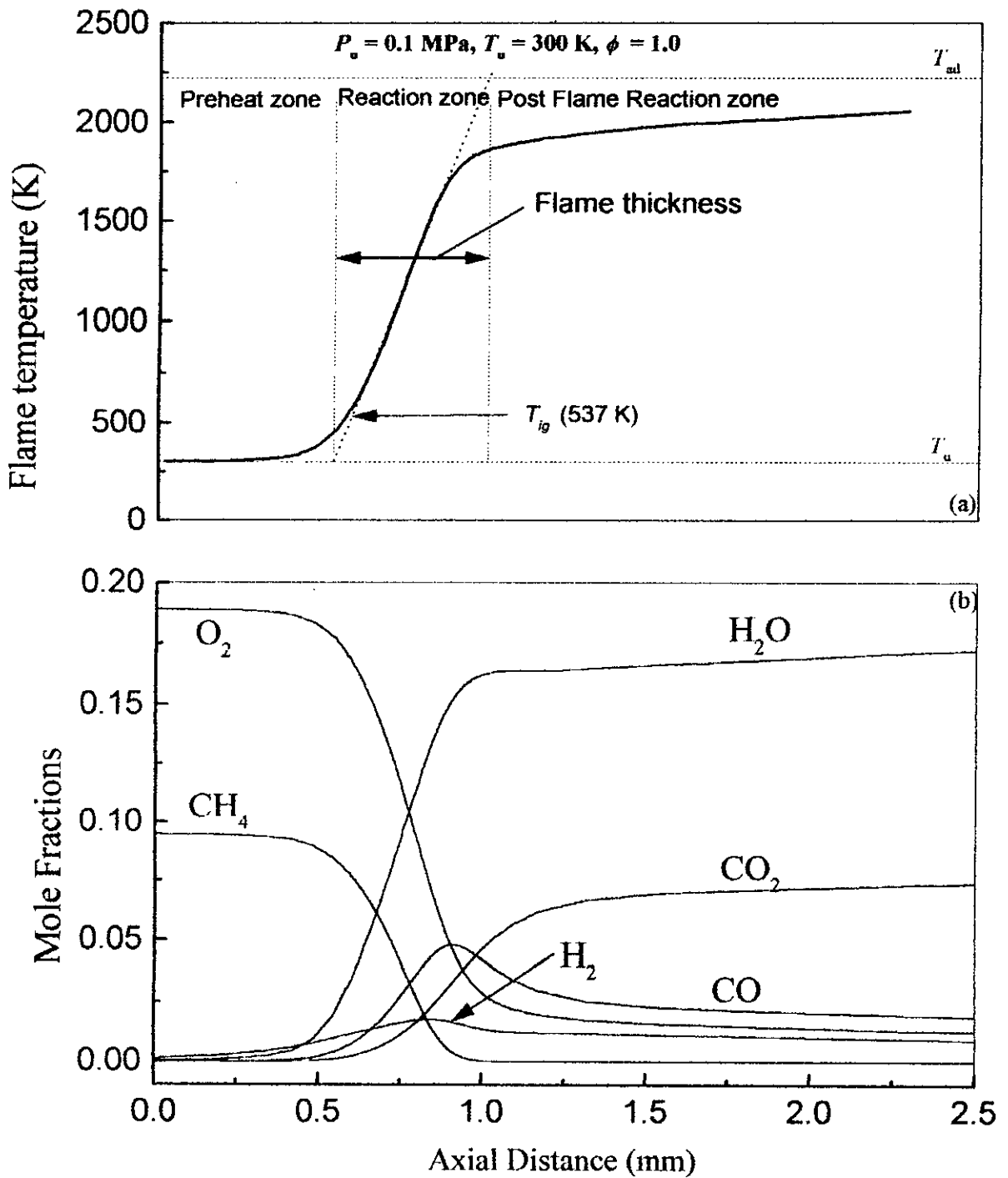


Fig. 3.5. Composition, temperature profile of one-dimensional, freely propagating methane-air mixture.

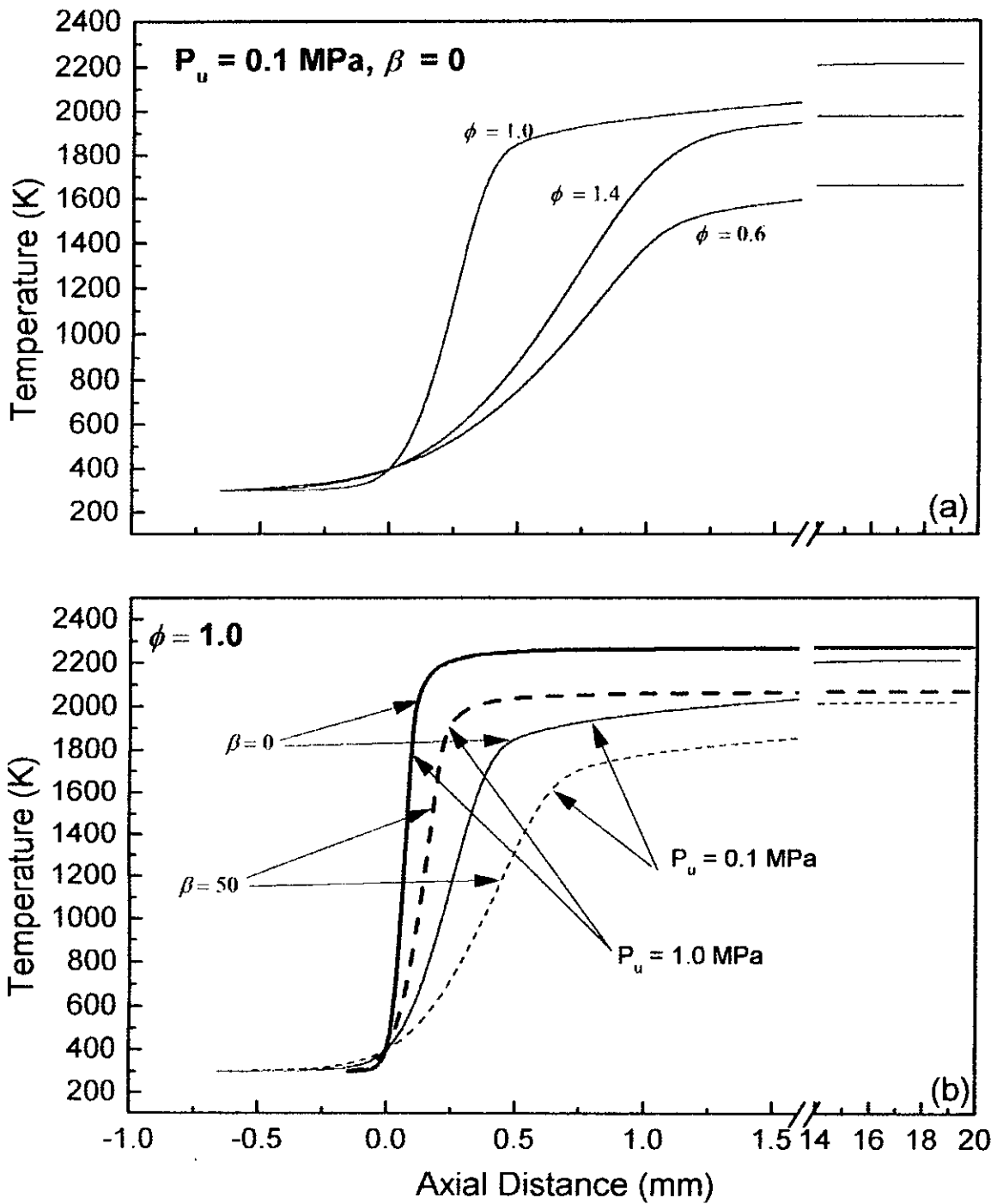


Fig. 3.6. Variation of temperature with axial distance, for different stoichiometry, composition of bio-gas and pressure.

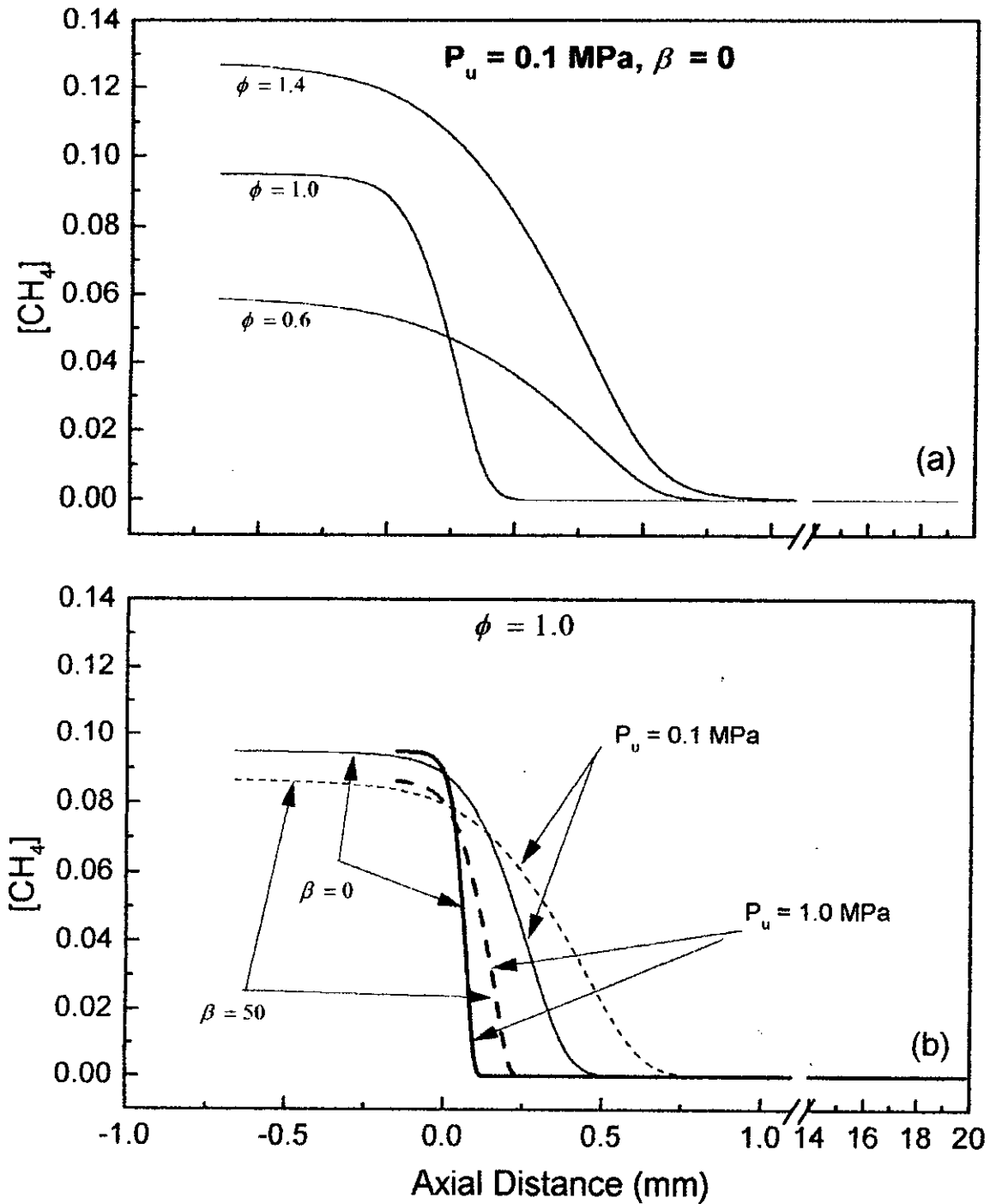


Fig. 3.7. Variation of $[CH_4]$ with axial distance, for different stoichiometry, composition of bio-gas and pressure.

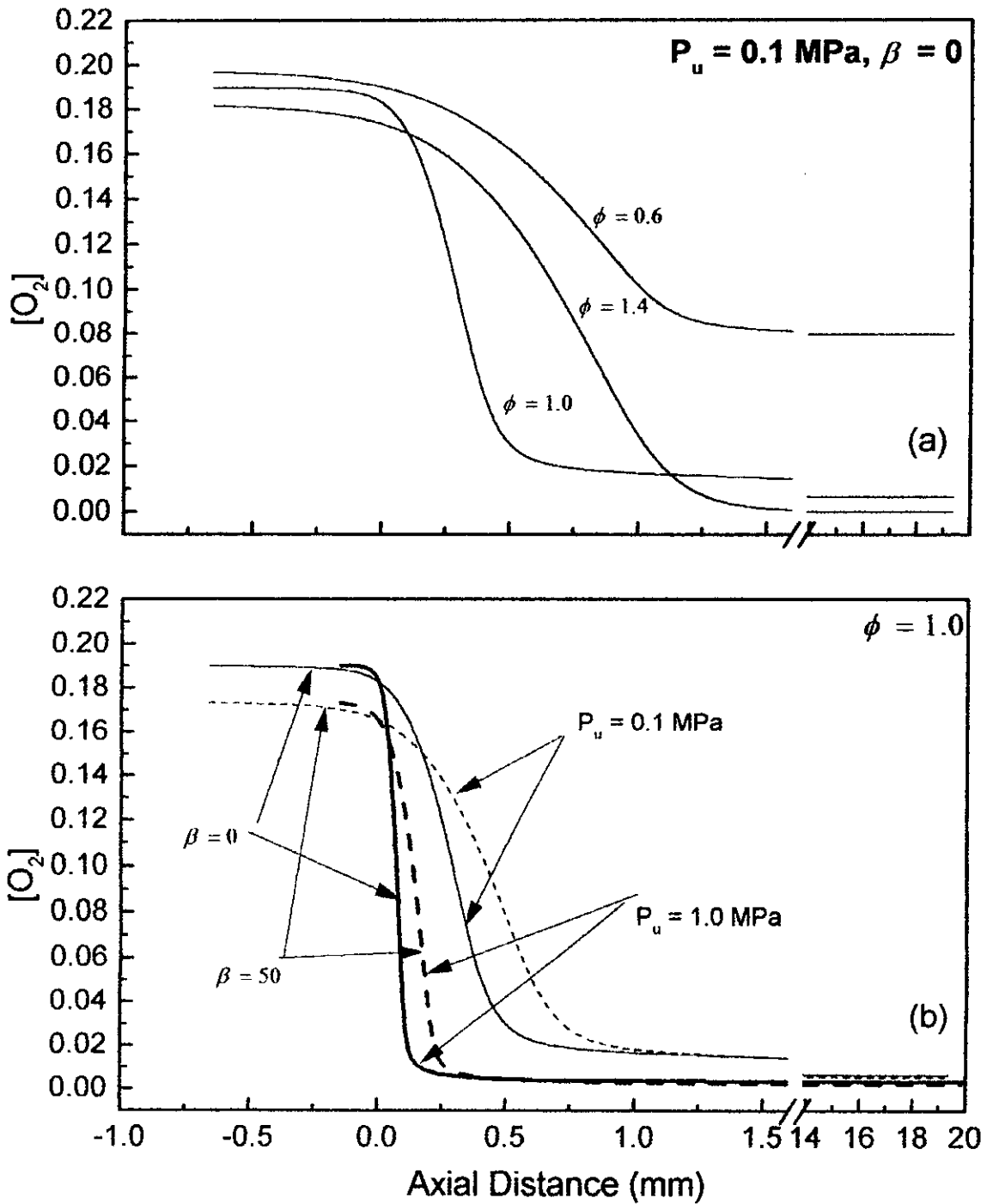


Fig. 3.8. Variation of $[O_2]$ with axial distance, for different stoichiometry, composition of bio-gas and pressure.

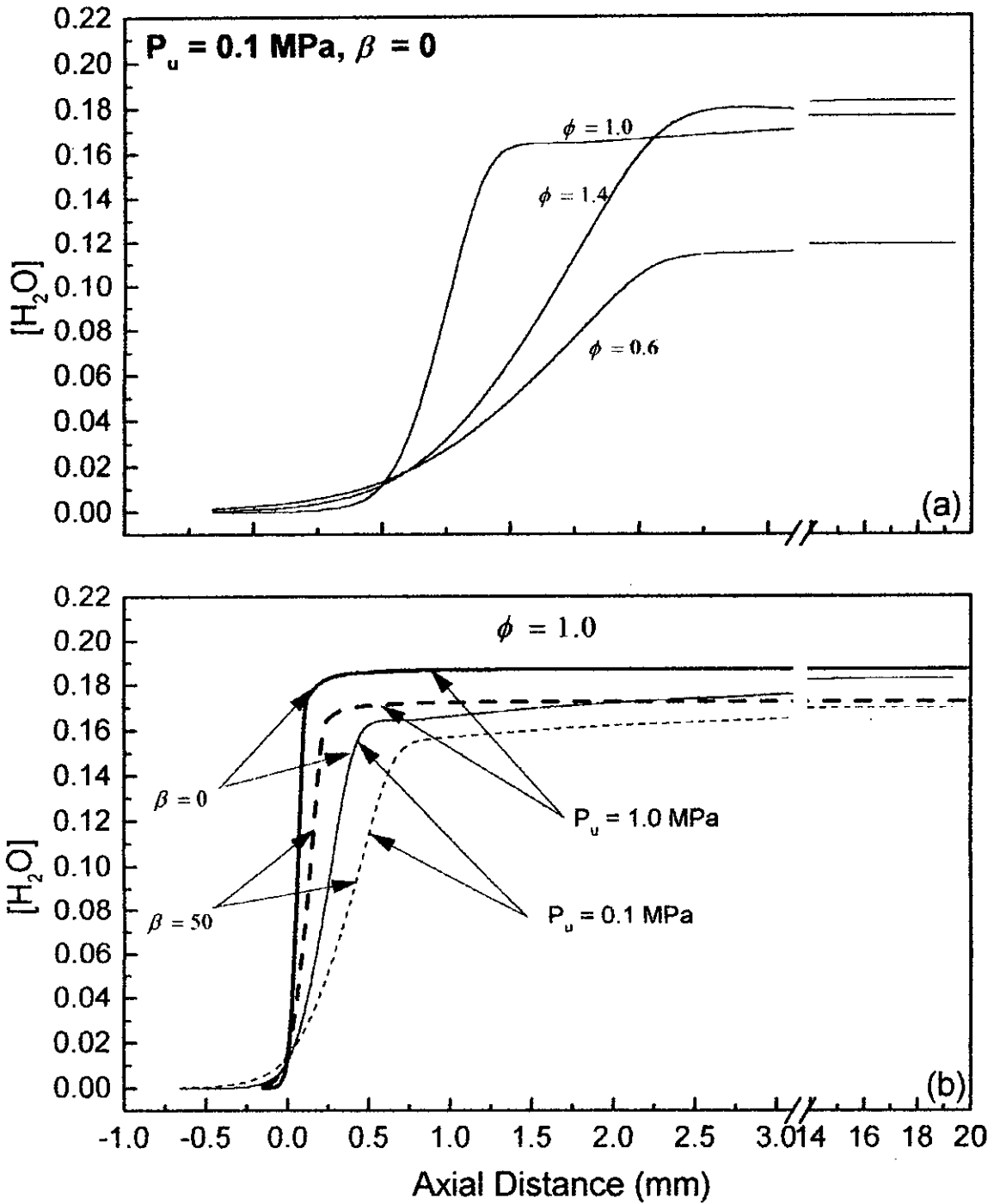


Fig. 3.9. Variation of $[H_2O]$ with axial distance, for different stoichiometry, composition of bio-gas and pressure.

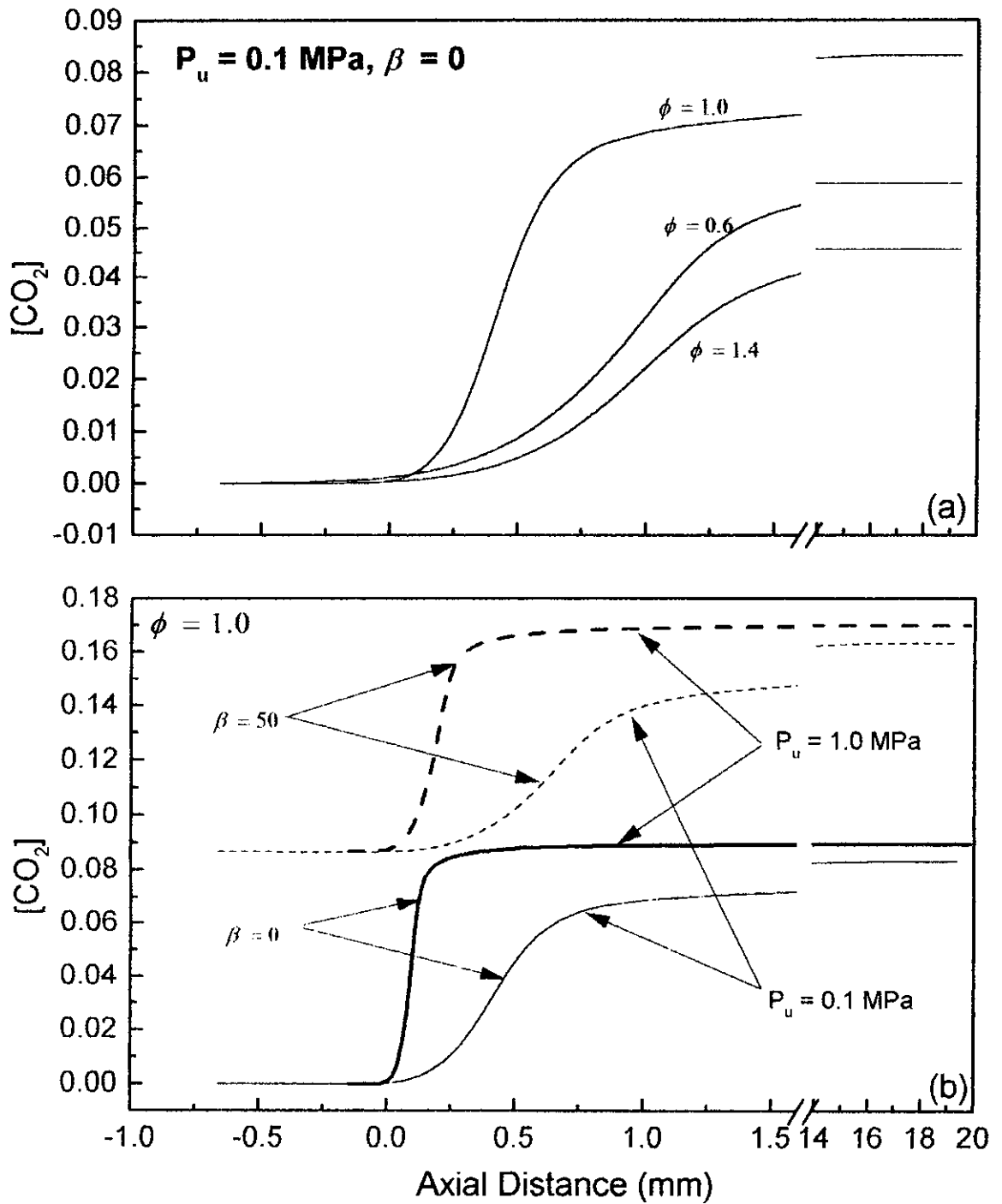


Fig. 3.10. Variation of $[CO_2]$ with axial distance, for different stoichiometry, composition of bio-gas and pressure.

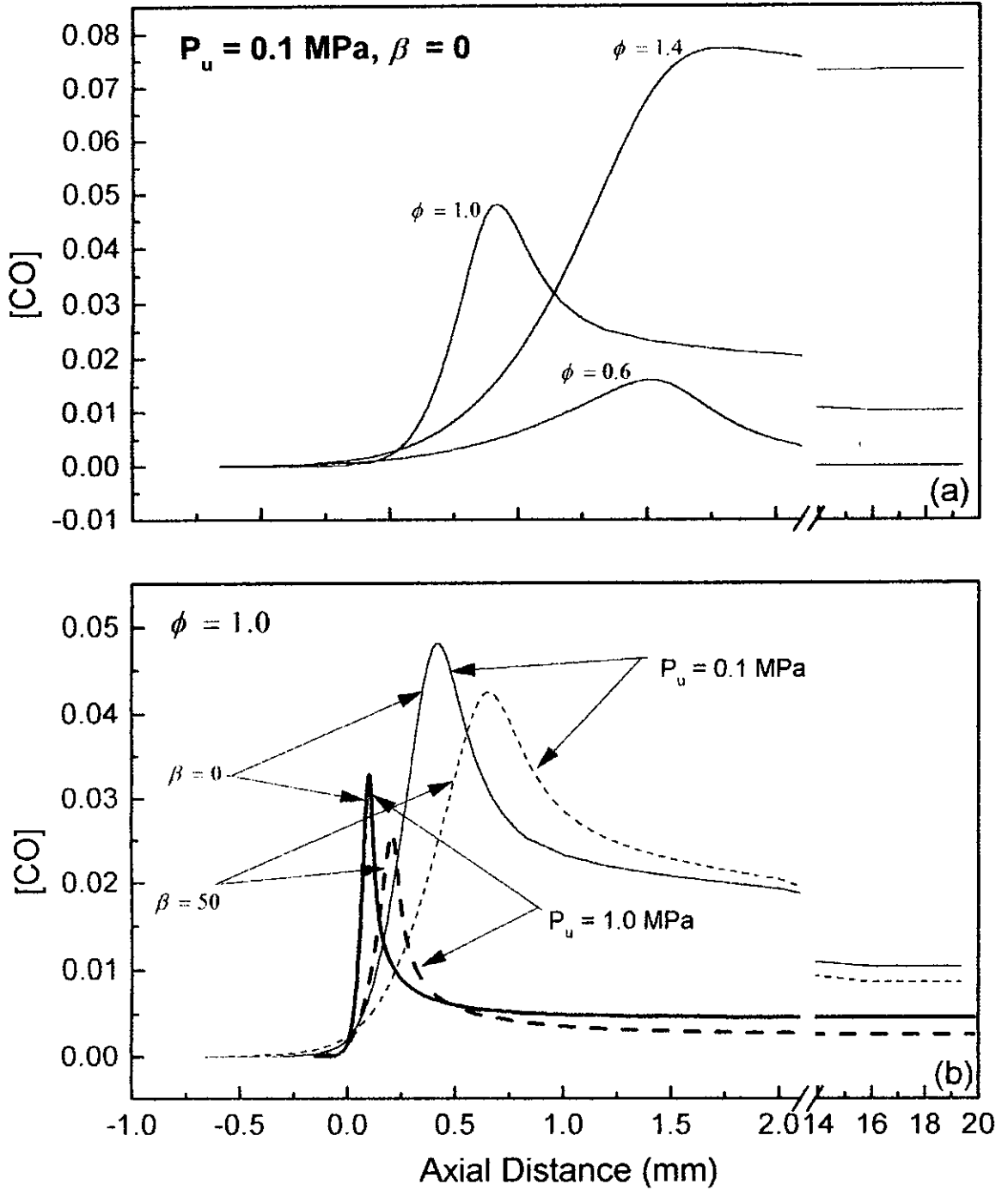


Fig. 3.11. Variation of [CO] with axial distance, for different stoichiometry, composition of bio-gas and pressure.

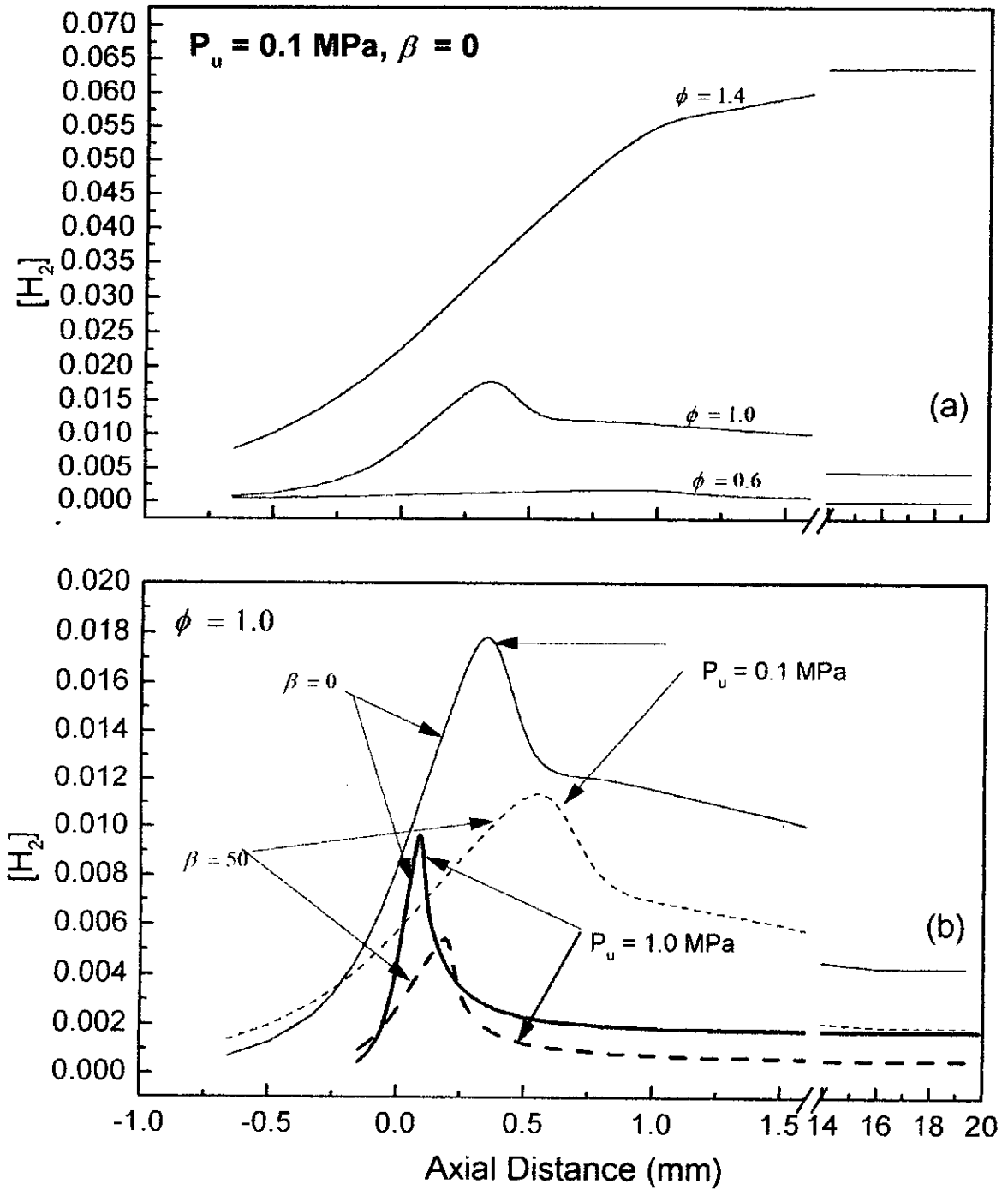


Fig. 3.12. Variation of $[H_2]$ with axial distance, for different stoichiometry, composition of bio-gas and pressure.

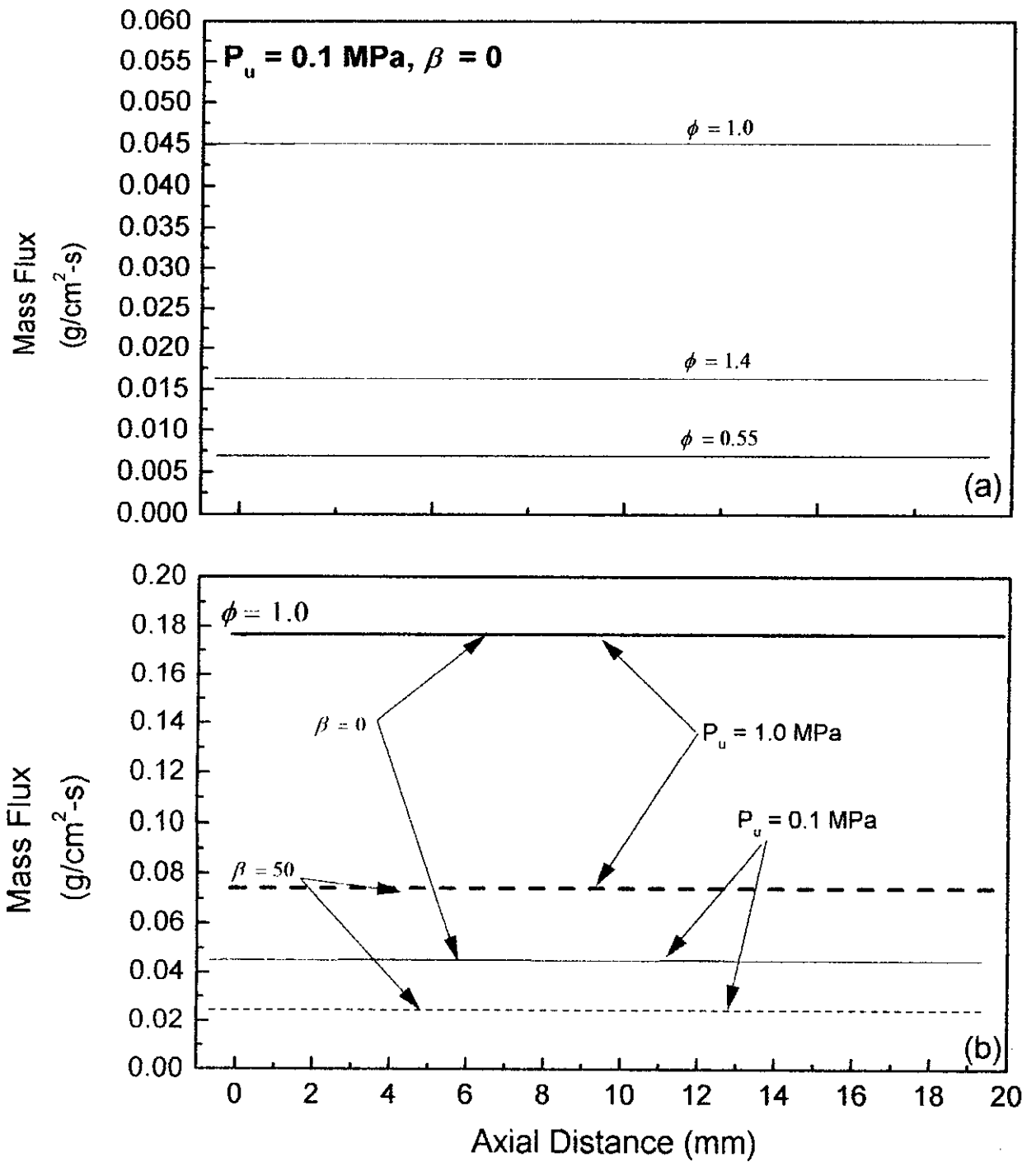


Fig. 3.13. Variation of mass flux, \dot{m} , with axial distance, for different stoichiometry, composition of bio-gas and pressure.

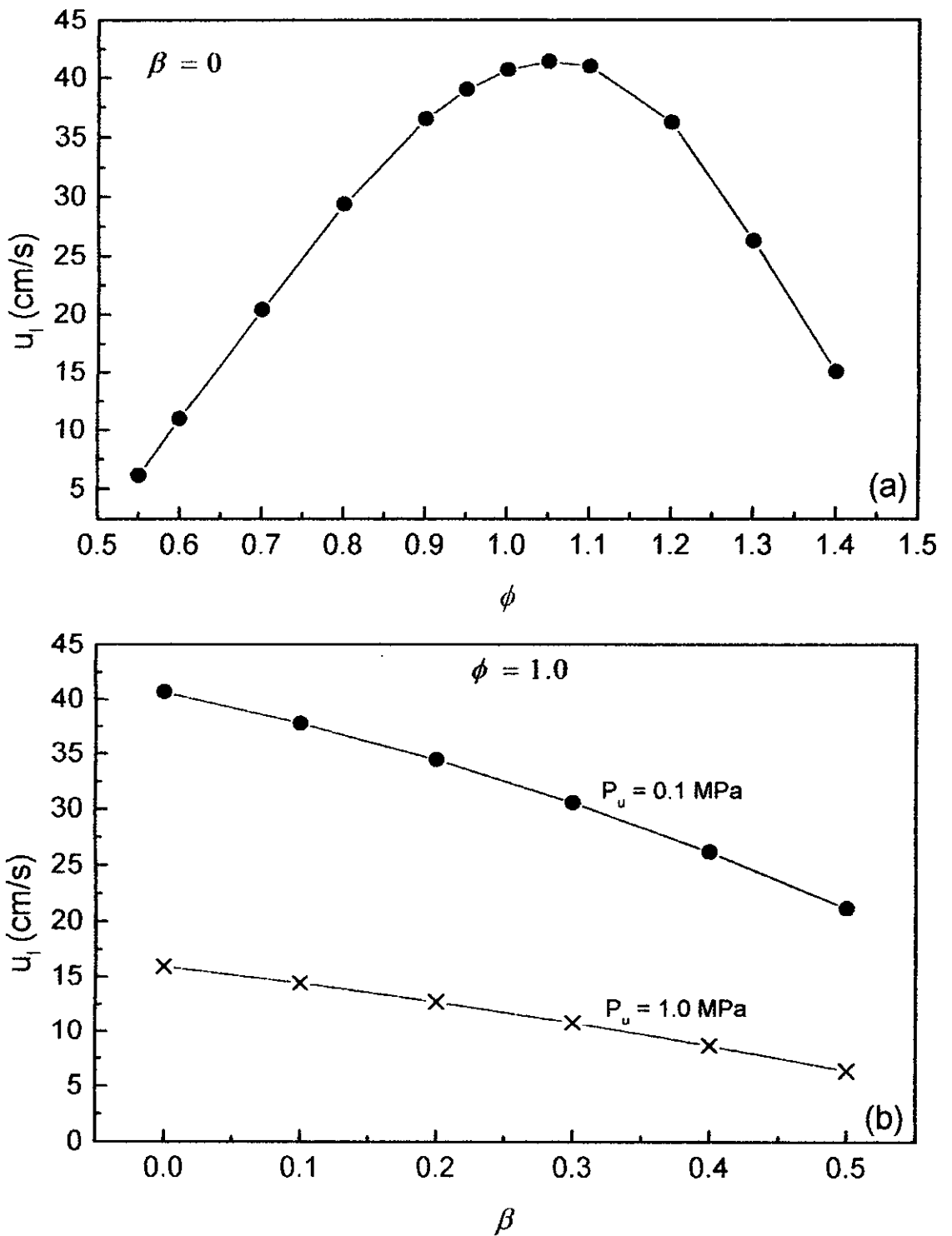


Fig. 3.14. Laminar burning velocities plotted against (a) ϕ , (b) β at different pressure.

Chapter 4

Conclusions

The present thesis comprises a numerical study of freely-propagating, one-dimensional, planar, adiabatic premixed flame propagation in methane, bio-gas and air premixture. The effect of the concentration of CO_2 in bio-gas mixtures are studied at different equivalence ratios at 300 K, at initial pressures of 0.1 and 1.0 MPa. In the present study, mole fraction of CO_2 are denoted by β and study is carried out for $\beta = 0, 0.1, 0.2, 0.3, 0.4$ and 0.5 .

The major conclusions of the study are:

- Heat release from a given premixture depends on its equivalence ratio. The heat release decreases with increase in CO_2 in bio-gas.
- The major products of lean combustion are H_2O , CO_2 , O_2 and N_2 , and for rich combustion the major products are H_2O , CO_2 , CO , H_2 and N_2 . Carbon-monoxide is a minor species in lean products, while O_2 is a minor product for rich cases.
- Dissociation of complete combustion products are important at higher temperatures and dissociation is suppressed by pressure. Hence, dissociation is found to be important for near stoichiometric condition combustions. Effect of pressure is also observed by the increase of flame temperature at these conditions.

- Water gas shift reaction is found very important in establishing the equilibria between CO , CO_2 , H_2 and H_2O .
- Flame thickness for the combustible mixtures considered in the present study are not negligible. For a given pressure, smallest flame thickness is associated with $\phi \approx 1.00$. Any increase in pressure results in decrease in the thickness. Flame thickness increases with the amount of CO_2 in bio-gas.
- Laminar burning velocities are strong function of ϕ , with its maximum value at $\phi = 1.05$. Increase in CO_2 in bio-gas results in lower burning velocities. Any increase in pressure also results in further decrease in the burning velocities.

The following observations are made with regard to the future works:

- Effect of other minor species, present in methane are bio-gas, on combustion.
- Flame radiation effect might be important for bio-gas combustion because of its slower speed.
- As all practical flames are nearly turbulent, study of turbulent combustion is important for optimum and efficient utilization of bio-gas.

Appendix A

Typical Output from EQUIL Code

CKLIB: Chemical Kinetics Library
CHEMKIN-II Version 4.9, April 1994
DOUBLE PRECISION

KEYWORD INPUT

REAC CO2 0.00
REAC CH4 0.5
REAC O2 1
REAC N2 3.76
CONH
CONP
TEMP 300
TEST 2230
PRES 0.9869
END

Constant pressure and enthalpy problem:

EQUIL: Chemkin interface for Stanjan-III
CHEMKIN-II Version 3.0, December 1992
DOUBLE PRECISION

WORKING SPACE REQUIREMENTS

	PROVIDED	REQUIRED
INTEGER	5000	896
REAL	5000	1930

STANJAN: Version 3.8C, May 1988
W. C. Reynolds, Stanford Univ.

	INITIAL STATE:	EQUILIBRIUM STATE:
P (atm)	9.8690E-01	9.8690E-01
T (K)	3.0000E+02	2.2321E+03
V (cm ³ /gm)	9.0263E+02	6.7656E+03
H (erg/gm)	-2.5560E+09	-2.5560E+09
U (erg/gm)	-3.4586E+09	-9.3215E+09
S (erg/gm-K)	7.2495E+07	9.8776E+07
W (gm/mole)	2.7633E+01	2.7431E+01

Mole Fractions

CH4	9.5057E-02	2.2645E-17
CO	0.0000E+00	8.7260E-03
CO2	0.0000E+00	8.5636E-02
H2O	0.0000E+00	1.8346E-01
O2	1.9011E-01	5.3151E-03
H2	0.0000E+00	3.5063E-03
H	0.0000E+00	3.9932E-04
O	0.0000E+00	2.4035E-04
OH	0.0000E+00	3.1208E-03
HO2	0.0000E+00	6.3723E-07
H2O2	0.0000E+00	5.0439E-08
C	0.0000E+00	2.2883E-17
CH	0.0000E+00	4.0777E-18
CH2	0.0000E+00	1.3224E-17
CH2 (S)	0.0000E+00	7.0905E-19
CH3	0.0000E+00	6.2720E-17
HCO	0.0000E+00	7.4962E-10
CH2O	0.0000E+00	1.8639E-11
CH2OH	0.0000E+00	6.7232E-17
CH3O	0.0000E+00	6.3229E-19
CH3OH	0.0000E+00	3.1441E-18
C2H	0.0000E+00	1.2005E-24
C2H2	0.0000E+00	8.8540E-22
C2H3	0.0000E+00	6.3849E-27
C2H4	0.0000E+00	5.9224E-27
C2H5	0.0000E+00	7.6620E-32
C2H6	0.0000E+00	4.2914E-33
HCCO	0.0000E+00	1.5009E-19
CH2CO	0.0000E+00	7.7569E-20
HCCOH	0.0000E+00	9.2942E-23
N2	7.1483E-01	7.0960E-01
AR	0.0000E+00	0.0000E+00

Appendix B

Methane Reaction Pathways

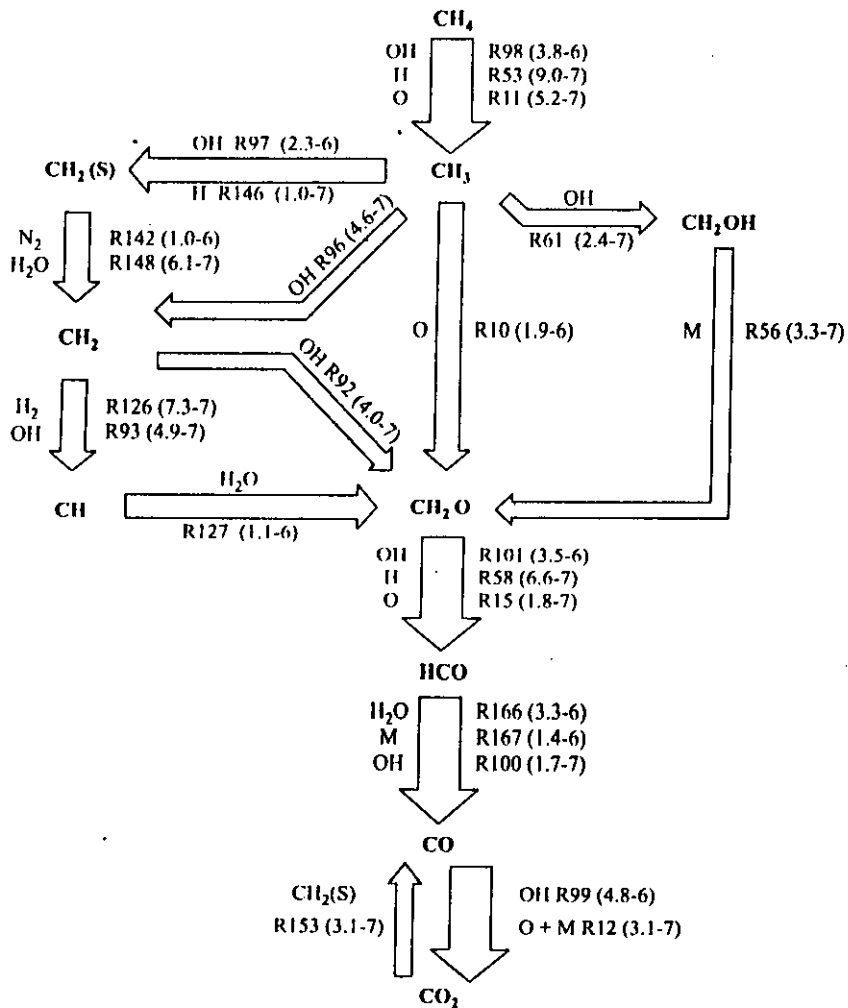


Fig. B.1. High temperature reaction pathway diagram for methane.

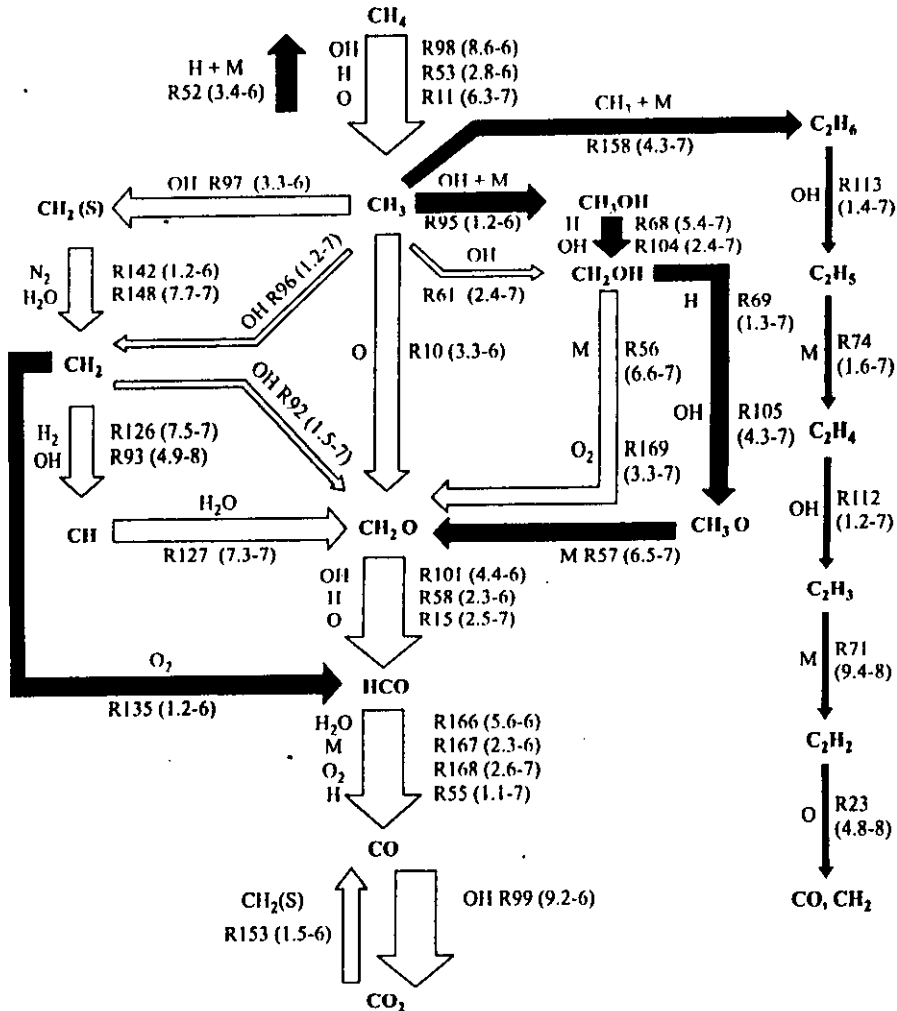


Fig. B.2. Low temperature reaction pathway diagram for methane.

Appendix C

GRI-Mech 1.2: Methane Reaction Mechanism

REACTIONS CONSIDERED				(k = A T**b exp(-E/RT))		
				A	b	E
1.	2O+M<=>O2+M			1.20E+17	-1.0	0.0
	H2	Enhanced by	2.400E+00			
	H2O	Enhanced by	1.540E+01			
	CH4	Enhanced by	2.000E+00			
	CO	Enhanced by	1.750E+00			
	CO2	Enhanced by	3.600E+00			
	C2H6	Enhanced by	3.000E+00			
	AR	Enhanced by	8.300E-01			
2.	O+H+M<=>OH+M			5.00E+17	-1.0	0.0
	H2	Enhanced by	2.000E+00			
	H2O	Enhanced by	6.000E+00			
	CH4	Enhanced by	2.000E+00			
	CO	Enhanced by	1.500E+00			
	CO2	Enhanced by	2.000E+00			
	C2H6	Enhanced by	3.000E+00			
	AR	Enhanced by	7.000E-01			
3.	O+H2<=>H+OH			5.00E+04	2.7	6290.0
4.	O+HO2<=>OH+O2			2.00E+13	0.0	0.0
5.	O+H2O2<=>OH+HO2			9.63E+06	2.0	4000.0
6.	O+CH<=>H+CO			5.70E+13	0.0	0.0
7.	O+CH2<=>H+HCO			8.00E+13	0.0	0.0
8.	O+CH2 (S) <=>H2+CO			1.50E+13	0.0	0.0
9.	O+CH2 (S) <=>H+HCO			1.50E+13	0.0	0.0
10.	O+CH3<=>H+CH2O			8.43E+13	0.0	0.0
11.	O+CH4<=>OH+CH3			1.02E+09	1.5	8600.0
12.	O+CO+M<=>CO2+M			6.02E+14	0.0	3000.0
	H2	Enhanced by	2.000E+00			
	O2	Enhanced by	6.000E+00			

H2O	Enhanced by	6.000E+00		
CH4	Enhanced by	2.000E+00		
CO	Enhanced by	1.500E+00		
CO2	Enhanced by	3.500E+00		
C2H6	Enhanced by	3.000E+00		
AR	Enhanced by	5.000E-01		
13. O+HCO<=>OH+CO			3.00E+13	0.0
14. O+HCO<=>H+CO2			3.00E+13	0.0
15. O+CH2O<=>OH+HCO			3.90E+13	0.0
16. O+CH2OH<=>OH+CH2O			1.00E+13	0.0
17. O+CH3O<=>OH+CH2O			1.00E+13	0.0
18. O+CH3OH<=>OH+CH2OH			3.88E+05	2.5
19. O+CH3OH<=>OH+CH3O			1.30E+05	2.5
20. O+C2H<=>CH+CO			5.00E+13	0.0
21. O+C2H2<=>H+HCCO			1.02E+07	2.0
22. O+C2H2<=>OH+C2H			4.60E+19	-1.4
23. O+C2H2<=>CO+CH2			1.02E+07	2.0
24. O+C2H3<=>H+CH2CO			3.00E+13	0.0
25. O+C2H4<=>CH3+HCO			1.92E+07	1.8
26. O+C2H5<=>CH3+CH2O			1.32E+14	0.0
27. O+C2H6<=>OH+C2H5			8.98E+07	1.9
28. O+HCCO<=>H+2CO			1.00E+14	0.0
29. O+CH2CO<=>OH+HCCO			1.00E+13	0.0
30. O+CH2CO<=>CH2+CO2			1.75E+12	0.0
31. O2+CO<=>O+CO2			2.50E+12	0.0
32. O2+CH2O<=>HO2+HCO			1.00E+14	0.0
33. H+O2+M<=>HO2+M			2.80E+18	-0.9
O2	Enhanced by	0.000E+00		
H2O	Enhanced by	0.000E+00		
CO	Enhanced by	7.500E-01		
CO2	Enhanced by	1.500E+00		
C2H6	Enhanced by	1.500E+00		
N2	Enhanced by	0.000E+00		
AR	Enhanced by	0.000E+00		
34. H+2O2<=>HO2+O2			3.00E+20	-1.7
35. H+O2+H2O<=>HO2+H2O			9.38E+18	-0.8
36. H+O2+N2<=>HO2+N2			3.75E+20	-1.7
37. H+O2+AR<=>HO2+AR			7.00E+17	-0.8
38. H+O2<=>O+OH			8.30E+13	0.0
39. 2H+M<=>H2+M			1.00E+18	-1.0
H2	Enhanced by	0.000E+00		
H2O	Enhanced by	0.000E+00		
CH4	Enhanced by	2.000E+00		
CO2	Enhanced by	0.000E+00		
C2H6	Enhanced by	3.000E+00		

AR	Enhanced by	6.300E-01			
40. 2H+H2<=>2H2			9.00E+16	-0.6	0.0
41. 2H+H2O<=>H2+H2O			6.00E+19	-1.2	0.0
42. 2H+CO2<=>H2+CO2			5.50E+20	-2.0	0.0
43. H+OH+M<=>H2O+M			2.20E+22	-2.0	0.0
H2	Enhanced by	7.300E-01			
H2O	Enhanced by	3.650E+00			
CH4	Enhanced by	2.000E+00			
C2H6	Enhanced by	3.000E+00			
AR	Enhanced by	3.800E-01			
44. H+HO2<=>O+H2O			3.97E+12	0.0	671.0
45. H+HO2<=>O2+H2			2.80E+13	0.0	1068.0
46. H+HO2<=>2OH			1.34E+14	0.0	635.0
47. H+H2O2<=>HO2+H2			1.21E+07	2.0	5200.0
48. H+H2O2<=>OH+H2O			1.00E+13	0.0	3600.0
49. H+CH<=>C+H2			1.10E+14	0.0	0.0
50. H+CH2 (+M) <=>CH3 (+M)			2.50E+16	-0.8	0.0
Low pressure limit:	0.32000E+28	-0.31400E+01	0.12300E+04		
TROE centering:	0.68000E+00	0.78000E+02	0.19950E+04	0.55900E+04	
H2	Enhanced by	2.000E+00			
H2O	Enhanced by	6.000E+00			
CH4	Enhanced by	2.000E+00			
CO	Enhanced by	1.500E+00			
CO2	Enhanced by	2.000E+00			
C2H6	Enhanced by	3.000E+00			
AR	Enhanced by	7.000E-01			
51. H+CH2 (S) <=>CH+H2			3.00E+13	0.0	0.0
52. H+CH3 (+M) <=>CH4 (+M)			1.27E+16	-0.6	383.0
Low pressure limit:	0.24770E+34	-0.47600E+01	0.24400E+04		
TROE centering:	0.78300E+00	0.74000E+02	0.29410E+04	0.69640E+04	
H2	Enhanced by	2.000E+00			
H2O	Enhanced by	6.000E+00			
CH4	Enhanced by	2.000E+00			
CO	Enhanced by	1.500E+00			
CO2	Enhanced by	2.000E+00			
C2H6	Enhanced by	3.000E+00			
AR	Enhanced by	7.000E-01			
53. H+CH4<=>CH3+H2			6.60E+08	1.6	10840.0
54. H+HCO (+M) <=>CH2O (+M)			1.09E+12	0.5	-260.0
Low pressure limit:	0.13500E+25	-0.25700E+01	0.14250E+04		
TROE centering:	0.78240E+00	0.27100E+03	0.27550E+04	0.65700E+04	
H2	Enhanced by	2.000E+00			
H2O	Enhanced by	6.000E+00			
CH4	Enhanced by	2.000E+00			
CO	Enhanced by	1.500E+00			

	CO2	Enhanced by	2.000E+00			
	C2H6	Enhanced by	3.000E+00			
	AR	Enhanced by	7.000E-01			
55.	H+HCO<=>H2+CO			7.34E+13	0.0	0.0
56.	H+CH2O(+M)<=>CH2OH(+M)			5.40E+11	0.5	3600.0
	Low pressure limit:	0.12700E+33	-0.48200E+01	0.65300E+04		
	TROE centering:	0.71870E+00	0.10300E+03	0.12910E+04	0.41600E+04	
	H2	Enhanced by	2.000E+00			
	H2O	Enhanced by	6.000E+00			
	CH4	Enhanced by	2.000E+00			
	CO	Enhanced by	1.500E+00			
	CO2	Enhanced by	2.000E+00			
	C2H6	Enhanced by	3.000E+00			
57.	H+CH2O(+M)<=>CH3O(+M)			5.40E+11	0.5	2600.0
	Low pressure limit:	0.22000E+31	-0.48000E+01	0.55600E+04		
	TROE centering:	0.75800E+00	0.94000E+02	0.15550E+04	0.42000E+04	
	H2	Enhanced by	2.000E+00			
	H2O	Enhanced by	6.000E+00			
	CH4	Enhanced by	2.000E+00			
	CO	Enhanced by	1.500E+00			
	CO2	Enhanced by	2.000E+00			
	C2H6	Enhanced by	3.000E+00			
58.	H+CH2O<=>HCO+H2			2.30E+10	1.1	3275.0
59.	H+CH2OH(+M)<=>CH3OH(+M)			1.80E+13	0.0	0.0
	Low pressure limit:	0.30000E+32	-0.48000E+01	0.33000E+04		
	TROE centering:	0.76790E+00	0.33800E+03	0.18120E+04	0.50810E+04	
	H2	Enhanced by	2.000E+00			
	H2O	Enhanced by	6.000E+00			
	CH4	Enhanced by	2.000E+00			
	CO	Enhanced by	1.500E+00			
	CO2	Enhanced by	2.000E+00			
	C2H6	Enhanced by	3.000E+00			
60.	H+CH2OH<=>H2+CH2O			2.00E+13	0.0	0.0
61.	H+CH2OH<=>OH+CH3			1.20E+13	0.0	0.0
62.	H+CH2OH<=>CH2(S)+H2O			6.00E+12	0.0	0.0
63.	H+CH3O(+M)<=>CH3OH(+M)			5.00E+13	0.0	0.0
	Low pressure limit:	0.86000E+29	-0.40000E+01	0.30250E+04		
	TROE centering:	0.89020E+00	0.14400E+03	0.28380E+04	0.45569E+05	
	H2	Enhanced by	2.000E+00			
	H2O	Enhanced by	6.000E+00			
	CH4	Enhanced by	2.000E+00			
	CO	Enhanced by	1.500E+00			
	CO2	Enhanced by	2.000E+00			
	C2H6	Enhanced by	3.000E+00			
64.	H+CH3O<=>H+CH2OH			3.40E+06	1.6	0.0

65.	H+CH3O<=>H2+CH2O		2.00E+13	0.0	0.0
66.	H+CH3O<=>OH+CH3		3.20E+13	0.0	0.0
67.	H+CH3O<=>CH2(S)+H2O		1.60E+13	0.0	0.0
68.	H+CH3OH<=>CH2OH+H2		1.70E+07	2.1	4870.0
69.	H+CH3OH<=>CH3O+H2		4.20E+06	2.1	4870.0
70.	H+C2H(+M)<=>C2H2(+M)		1.00E+17	-1.0	0.0
	Low pressure limit:	0.37500E+34	-0.48000E+01	0.19000E+04	
	TROE centering:	0.64640E+00	0.13200E+03	0.13150E+04	0.55660E+04
	H2	Enhanced by	2.000E+00		
	H2O	Enhanced by	6.000E+00		
	CH4	Enhanced by	2.000E+00		
	CO	Enhanced by	1.500E+00		
	CO2	Enhanced by	2.000E+00		
	C2H6	Enhanced by	3.000E+00		
	AR	Enhanced by	7.000E-01		
71.	H+C2H2(+M)<=>C2H3(+M)		5.60E+12	0.0	2400.0
	Low pressure limit:	0.38000E+41	-0.72700E+01	0.72200E+04	
	TROE centering:	0.75070E+00	0.98500E+02	0.13020E+04	0.41670E+04
	H2	Enhanced by	2.000E+00		
	H2O	Enhanced by	6.000E+00		
	CH4	Enhanced by	2.000E+00		
	CO	Enhanced by	1.500E+00		
	CO2	Enhanced by	2.000E+00		
	C2H6	Enhanced by	3.000E+00		
	AR	Enhanced by	7.000E-01		
72.	H+C2H3(+M)<=>C2H4(+M)		6.08E+12	0.3	280.0
	Low pressure limit:	0.14000E+31	-0.38600E+01	0.33200E+04	
	TROE centering:	0.78200E+00	0.20750E+03	0.26630E+04	0.60950E+04
	H2	Enhanced by	2.000E+00		
	H2O	Enhanced by	6.000E+00		
	CH4	Enhanced by	2.000E+00		
	CO	Enhanced by	1.500E+00		
	CO2	Enhanced by	2.000E+00		
	C2H6	Enhanced by	3.000E+00		
	AR	Enhanced by	7.000E-01		
73.	H+C2H3<=>H2+C2H2		3.00E+13	0.0	0.0
74.	H+C2H4(+M)<=>C2H5(+M)		1.08E+12	0.5	1820.0
	Low pressure limit:	0.12000E+43	-0.76200E+01	0.69700E+04	
	TROE centering:	0.97530E+00	0.21000E+03	0.98400E+03	0.43740E+04
	H2	Enhanced by	2.000E+00		
	H2O	Enhanced by	6.000E+00		
	CH4	Enhanced by	2.000E+00		
	CO	Enhanced by	1.500E+00		
	CO2	Enhanced by	2.000E+00		
	C2H6	Enhanced by	3.000E+00		

	AR	Enhanced by	7.000E-01			
75.	H+C2H4<=>C2H3+H2			1.32E+06	2.5	12240.0
76.	H+C2H5(+M)<=>C2H6(+M)			5.21E+17	-1.0	1580.0
	Low pressure limit:	0.19900E+42	-0.70800E+01	0.66850E+04		
	TROE centering:	0.84220E+00	0.12500E+03	0.22190E+04	0.68820E+04	
	H2	Enhanced by	2.000E+00			
	H2O	Enhanced by	6.000E+00			
	CH4	Enhanced by	2.000E+00			
	CO	Enhanced by	1.500E+00			
	CO2	Enhanced by	2.000E+00			
	C2H6	Enhanced by	3.000E+00			
	AR	Enhanced by	7.000E-01			
77.	H+C2H5<=>H2+C2H4			2.00E+12	0.0	0.0
78.	H+C2H6<=>C2H5+H2			1.15E+08	1.9	7530.0
79.	H+HCCO<=>CH2(S)+CO			1.00E+14	0.0	0.0
80.	H+CH2CO<=>HCCO+H2			5.00E+13	0.0	8000.0
81.	H+CH2CO<=>CH3+CO			1.13E+13	0.0	3428.0
82.	H+HCCOH<=>H+CH2CO			1.00E+13	0.0	0.0
83.	H2+CO(+M)<=>CH2O(+M)			4.30E+07	1.5	79600.0
	Low pressure limit:	0.50700E+28	-0.34200E+01	0.84350E+05		
	TROE centering:	0.93200E+00	0.19700E+03	0.15400E+04	0.10300E+05	
	H2	Enhanced by	2.000E+00			
	H2O	Enhanced by	6.000E+00			
	CH4	Enhanced by	2.000E+00			
	CO	Enhanced by	1.500E+00			
	CO2	Enhanced by	2.000E+00			
	C2H6	Enhanced by	3.000E+00			
	AR	Enhanced by	7.000E-01			
84.	OH+H2<=>H+H2O			2.16E+08	1.5	3430.0
85.	2OH(+M)<=>H2O2(+M)			7.40E+13	-0.4	0.0
	Low pressure limit:	0.23000E+19	-0.90000E+00	-0.17000E+04		
	TROE centering:	0.73460E+00	0.94000E+02	0.17560E+04	0.51820E+04	
	H2	Enhanced by	2.000E+00			
	H2O	Enhanced by	6.000E+00			
	CH4	Enhanced by	2.000E+00			
	CO	Enhanced by	1.500E+00			
	CO2	Enhanced by	2.000E+00			
	C2H6	Enhanced by	3.000E+00			
	AR	Enhanced by	7.000E-01			
86.	2OH<=>O+H2O			3.57E+04	2.4	-2110.0
87.	OH+HO2<=>O2+H2O			2.90E+13	0.0	-500.0
88.	OH+H2O2<=>HO2+H2O			1.75E+12	0.0	320.0
	Declared duplicate reaction...					
89.	OH+H2O2<=>HO2+H2O			5.80E+14	0.0	9560.0
	Declared duplicate reaction...					

90.	OH+C<=>H+CO	5.00E+13	0.0	0.0
91.	OH+CH<=>H+HCO	3.00E+13	0.0	0.0
92.	OH+CH2<=>H+CH2O	2.00E+13	0.0	0.0
93.	OH+CH2<=>CH+H2O	1.13E+07	2.0	3000.0
94.	OH+CH2(S)<=>H+CH2O	3.00E+13	0.0	0.0
95.	OH+CH3(+M)<=>CH3OH(+M)	6.30E+13	0.0	0.0
	Low pressure limit:	0.27000E+39	-0.63000E+01	0.31000E+04
	TROE centering:	0.21050E+00	0.83500E+02	0.53980E+04 0.83700E+04
	H2	Enhanced by	2.000E+00	
	H2O	Enhanced by	6.000E+00	
	CH4	Enhanced by	2.000E+00	
	CO	Enhanced by	1.500E+00	
	CO2	Enhanced by	2.000E+00	
	C2H6	Enhanced by	3.000E+00	
96.	OH+CH3<=>CH2+H2O	5.60E+07	1.6	5420.0
97.	OH+CH3<=>CH2(S)+H2O	2.50E+13	0.0	0.0
98.	OH+CH4<=>CH3+H2O	1.00E+08	1.6	3120.0
99.	OH+CO<=>H+CO2	4.76E+07	1.2	70.0
100.	OH+HCO<=>H2O+CO	5.00E+13	0.0	0.0
101.	OH+CH2O<=>HCO+H2O	3.43E+09	1.2	-447.0
102.	OH+CH2OH<=>H2O+CH2O	5.00E+12	0.0	0.0
103.	OH+CH3O<=>H2O+CH2O	5.00E+12	0.0	0.0
104.	OH+CH3OH<=>CH2OH+H2O	1.44E+06	2.0	-840.0
105.	OH+CH3OH<=>CH3O+H2O	6.30E+06	2.0	1500.0
106.	OH+C2H<=>H+HCCO	2.00E+13	0.0	0.0
107.	OH+C2H2<=>H+CH2CO	2.18E-04	4.5	-1000.0
108.	OH+C2H2<=>H+HCCOH	5.04E+05	2.3	13500.0
109.	OH+C2H2<=>C2H+H2O	3.37E+07	2.0	14000.0
110.	OH+C2H2<=>CH3+CO	4.83E-04	4.0	-2000.0
111.	OH+C2H3<=>H2O+C2H2	5.00E+12	0.0	0.0
112.	OH+C2H4<=>C2H3+H2O	3.60E+06	2.0	2500.0
113.	OH+C2H6<=>C2H5+H2O	3.54E+06	2.1	870.0
114.	OH+CH2CO<=>HCCO+H2O	7.50E+12	0.0	2000.0
115.	2HO2<=>O2+H2O2	1.30E+11	0.0	-1630.0
	Declared duplicate reaction...			
116.	2HO2<=>O2+H2O2	4.20E+14	0.0	12000.0
	Declared duplicate reaction...			
117.	HO2+CH2<=>OH+CH2O	2.00E+13	0.0	0.0
118.	HO2+CH3<=>O2+CH4	1.00E+12	0.0	0.0
119.	HO2+CH3<=>OH+CH3O	2.00E+13	0.0	0.0
120.	HO2+CO<=>OH+CO2	1.50E+14	0.0	23600.0
121.	HO2+CH2O<=>HCO+H2O2	1.00E+12	0.0	8000.0
122.	C+O2<=>O+CO	5.80E+13	0.0	576.0
123.	C+CH2<=>H+C2H	5.00E+13	0.0	0.0
124.	C+CH3<=>H+C2H2	5.00E+13	0.0	0.0

125.	CH+O2<=>O+HCO	3.30E+13	0.0	0.0
126.	CH+H2<=>H+CH2	1.11E+08	1.8	1670.0
127.	CH+H2O<=>H+CH2O	5.71E+12	0.0	-755.0
128.	CH+CH2<=>H+C2H2	4.00E+13	0.0	0.0
129.	CH+CH3<=>H+C2H3	3.00E+13	0.0	0.0
130.	CH+CH4<=>H+C2H4	6.00E+13	0.0	0.0
131.	CH+CO (+M) <=>HCCO (+M)	5.00E+13	0.0	0.0
	Low pressure limit:	0.26900E+29	-0.37400E+01	0.19360E+04
	TROE centering:	0.57570E+00	0.23700E+03	0.16520E+04 0.50690E+04
	H2	Enhanced by	2.000E+00	
	H2O	Enhanced by	6.000E+00	
	CH4	Enhanced by	2.000E+00	
	CO	Enhanced by	1.500E+00	
	CO2	Enhanced by	2.000E+00	
	C2H6	Enhanced by	3.000E+00	
	AR	Enhanced by	7.000E-01	
132.	CH+CO2<=>HCO+CO	3.40E+12	0.0	690.0
133.	CH+CH2O<=>H+CH2CO	9.46E+13	0.0	-515.0
134.	CH+HCCO<=>CO+C2H2	5.00E+13	0.0	0.0
135.	CH2+O2<=>OH+HCO	1.32E+13	0.0	1500.0
136.	CH2+H2<=>H+CH3	5.00E+05	2.0	7230.0
137.	2CH2<=>H2+C2H2	3.20E+13	0.0	0.0
138.	CH2+CH3<=>H+C2H4	4.00E+13	0.0	0.0
139.	CH2+CH4<=>2CH3	2.46E+06	2.0	8270.0
140.	CH2+CO (+M) <=>CH2CO (+M)	8.10E+11	0.5	4510.0
	Low pressure limit:	0.26900E+34	-0.51100E+01	0.70950E+04
	TROE centering:	0.59070E+00	0.27500E+03	0.12260E+04 0.51850E+04
	H2	Enhanced by	2.000E+00	
	H2O	Enhanced by	6.000E+00	
	CH4	Enhanced by	2.000E+00	
	CO	Enhanced by	1.500E+00	
	CO2	Enhanced by	2.000E+00	
	C2H6	Enhanced by	3.000E+00	
	AR	Enhanced by	7.000E-01	
141.	CH2+HCCO<=>C2H3+CO	3.00E+13	0.0	0.0
142.	CH2 (S) +N2<=>CH2+N2	1.50E+13	0.0	600.0
143.	CH2 (S) +AR<=>CH2+AR	9.00E+12	0.0	600.0
144.	CH2 (S) +O2<=>H+OH+CO	2.80E+13	0.0	0.0
145.	CH2 (S) +O2<=>CO+H2O	1.20E+13	0.0	0.0
146.	CH2 (S) +H2<=>CH3+H	7.00E+13	0.0	0.0
147.	CH2 (S) +H2O (+M) <=>CH3OH (+M)	2.00E+13	0.0	0.0
	Low pressure limit:	0.27000E+39	-0.63000E+01	0.31000E+04
	TROE centering:	0.15070E+00	0.13400E+03	0.23830E+04 0.72650E+04
	H2	Enhanced by	2.000E+00	
	H2O	Enhanced by	6.000E+00	

CH4	Enhanced by	2.000E+00		
CO	Enhanced by	1.500E+00		
CO2	Enhanced by	2.000E+00		
C2H6	Enhanced by	3.000E+00		
148. CH2 (S) +H2O<=>CH2+H2O		3.00E+13	0.0	0.0
149. CH2 (S) +CH3<=>H+C2H4		1.20E+13	0.0	-570.0
150. CH2 (S) +CH4<=>2CH3		1.60E+13	0.0	-570.0
151. CH2 (S) +CO<=>CH2+CO		9.00E+12	0.0	0.0
152. CH2 (S) +CO2<=>CH2+CO2		7.00E+12	0.0	0.0
153. CH2 (S) +CO2<=>CO+CH2O		1.40E+13	0.0	0.0
154. CH2 (S) +C2H6<=>CH3+C2H5		4.00E+13	0.0	-550.0
155. CH3+O2<=>O+CH3O		2.68E+13	0.0	28800.0
156. CH3+O2<=>OH+CH2O		3.60E+10	0.0	8940.0
157. CH3+H2O2<=>HO2+CH4		2.45E+04	2.5	5180.0
158. 2CH3 (+M) <=>C2H6 (+M)		2.12E+16	-1.0	620.0
Low pressure limit:	0.17700E+51	-0.96700E+01	0.62200E+04	
TROE centering:	0.53250E+00	0.15100E+03	0.10380E+04	0.49700E+04
H2	Enhanced by	2.000E+00		
H2O	Enhanced by	6.000E+00		
CH4	Enhanced by	2.000E+00		
CO	Enhanced by	1.500E+00		
CO2	Enhanced by	2.000E+00		
C2H6	Enhanced by	3.000E+00		
AR	Enhanced by	7.000E-01		
159. 2CH3<=>H+C2H5		4.99E+12	0.1	10600.0
160. CH3+HCO<=>CH4+CO		2.65E+13	0.0	0.0
161. CH3+CH2O<=>HCO+CH4		3.32E+03	2.8	5860.0
162. CH3+CH3OH<=>CH2OH+CH4		3.00E+07	1.5	9940.0
163. CH3+CH3OH<=>CH3O+CH4		1.00E+07	1.5	9940.0
164. CH3+C2H4<=>C2H3+CH4		2.27E+05	2.0	9200.0
165. CH3+C2H6<=>C2H5+CH4		6.14E+06	1.7	10450.0
166. HCO+H2O<=>H+CO+H2O		2.24E+18	-1.0	17000.0
167. HCO+M<=>H+CO+M		1.87E+17	-1.0	17000.0
H2	Enhanced by	2.000E+00		
H2O	Enhanced by	0.000E+00		
CH4	Enhanced by	2.000E+00		
CO	Enhanced by	1.500E+00		
CO2	Enhanced by	2.000E+00		
C2H6	Enhanced by	3.000E+00		
168. HCO+O2<=>HO2+CO		7.60E+12	0.0	400.0
169. CH2OH+O2<=>HO2+CH2O		1.80E+13	0.0	900.0
170. CH3O+O2<=>HO2+CH2O		4.28E-13	7.6	-3530.0
171. C2H+O2<=>HCO+CO		5.00E+13	0.0	1500.0
172. C2H+H2<=>H+C2H2		4.07E+05	2.4	200.0
173. C2H3+O2<=>HCO+CH2O		3.98E+12	0.0	-240.0

174.	$C_2H_4 (+M) \rightleftharpoons H_2 + C_2H_2 (+M)$		$8.00E+12$	0.4	88770.0
	Low pressure limit:	$0.70000E+51$	$-0.93100E+01$	$0.99860E+05$	
	TROE centering:	$0.73450E+00$	$0.18000E+03$	$0.10350E+04$	$0.54170E+04$
	H2	Enhanced by	$2.000E+00$		
	H2O	Enhanced by	$6.000E+00$		
	CH4	Enhanced by	$2.000E+00$		
	CO	Enhanced by	$1.500E+00$		
	CO2	Enhanced by	$2.000E+00$		
	C2H6	Enhanced by	$3.000E+00$		
	AR	Enhanced by	$7.000E-01$		
175.	$C_2H_5 + O_2 \rightleftharpoons HO_2 + C_2H_4$		$8.40E+11$	0.0	3875.0
176.	$HCCO + O_2 \rightleftharpoons OH + 2CO$		$1.60E+12$	0.0	854.0
177.	$2HCCO \rightleftharpoons 2CO + C_2H_2$		$1.00E+13$	0.0	0.0

NOTE: A units mole-cm-sec-K, E units cal/mole

Appendix D

Input of PREMIX INPUT

```
/ flame configuration, burner stabilized with specified temperature
/RSTR
FREE
ENRG
/ in the event of a Newton failure, take 100 timesteps of 1.E-6
TIME 100 1.E-7
/ begin on a uniform mesh of 6 points
NPTS 10
/ definition of the computational interval
XEND 10.
XSTR -2.
XCEN .1
WMIX 1.
/ pressure and inlet mass flow rate
PRES 1.01 (atmospheres)
FLRT .4 (g/cm**2-sec)
TFIX 400
/ adaptive mesh criteria
GRAD 0.5
CURV 0.5
/ unreacted mole fractions
MOLE
REAC CH4 0.0950
REAC O2 0.1896
REAC N2 0.7067
REAC AR 0.0084
/ estimated products
PROD H2O 0.19
PROD N2 0.7067
PROD CO2 0.095
PROD AR 0.0084
/ estimated intermediate mole fractions
```

```
INTM  H2  .01
INTM  H   .02
INTM  O   .0001
INTM  OH  .001
INTM  HO2 .0001
/INTM  H2O2 .0001
/INTM  C   .000001
INTM  CH  .00001
/INTM  CH2 .0001
/INTM  CH3 .0005
INTM  CO  .08
INTM  HCO .00001
INTM  CH2O .001
/INTM  CH2OH .00001
/INTM  CH3O .00001
/INTM  CH3OH .00001
/INTM  HCCO .0001
/INTM  CH2CO .0001
/INTM  HCCOH .0001
/  tolerances for the Newton iteration
ATOL  1.E-9
RTOL  1.E-4
/  tolerances for the time step Newton iteration
ATIM  1.E-5
RTIM  1.E-5
/  print control
PRNT  1
/  given temperature profile
TEMP  -2.    298
TEMP  0.     298.
TEMP  .03    300.
TEMP  .05    400.
TEMP  .06    766.
TEMP  .07    1512.
TEMP  .08    1892.
TEMP  .09    2000.
TEMP  .1     2030.
TEMP  .2     2111.
TEMP  .35    2190.
TEMP  10.0   2190.
END
```


References

- Bari, S., W. K. Biswas, and M. Z. Haq (1994). Performance of Diesel Engine with Biogas/Diesel Dual Fueling. In *The First Annual Paper Meet*, pp. 311–318. The Institutions of Engineers, Bangladesh.
- Bird, R. B., W. E. Stewart, and E. N. Lightfoot (1960). *Transport Phenomena*. John Wiley & Sons.
- Borman, G. L. and K. W. Ragland (1998). *Combustion Engineering*. McGraw-Hill Book Company.
- Burcat, A. and B. McBride (1997). 1997 Ideal Gas Thermodynamic Data for Combustion and Air-Pollution Use. Technical Report TAE-804, Technion - Israel Institute of Technology.
- De Nevers (2000). *Air Pollution Control Engineering*. McGraw-Hill Book Company.
- Ferguson, C. R. (1986). *Internal Combustion Engines: Applied Thermosciences*. John Wiley & Sons.
- Frenklach, M., H. Wang, M. Goldenberg, G. P. Smith, D. M. Golden, C. T. Bowman, R. K. Hanson, W. C. Gardiner, and V. Lissuanski (1995, November). GRI-MECH An Optimized Detailed Chemical Reaction Mechanism for Methane Combustion. Technical Report GRI-95/0058, Gas Research Institute.
- Glassman, I. (1996). *Combustion* (Third ed.). San Diego, California: Academic Press.

- Goodger, E. M. (1980). *Alternative Fuels - Chemical Energy Resources*. Macmillan Press Ltd.
- Gu, X. J., M. Z. Haq, M. Lawes, and R. Woolley (2000). Laminar Burning Velocity and Markstein Lengths of Methane-Air Mixtures. *Combust. Flame* **121**, 41–58.
- Heywood, J. B. (1988). *Internal Combustion Engine Fundamentals*. McGraw-Hill Book Company.
- Kee, R. J., G. Dixon-Lewis, J. Warnatz, M. E. Coltrin, and J. A. Miller (1986). A FORTRAN Computer Code Package for the Evolution of Gas-Phase Multicomponent Transport Properties. Technical Report SAND86-8246, Sandia National Laboratories, Livermore, CA.
- Kee, R. J., J. F. Grcar, M. D. Smooke, and J. A. Miller (1985). A FORTRAN Program for Modeling Steady Laminar One-dimensional Premixed Flames. Technical Report SAND85-8240, Sandia National Laboratories, Livermore, CA.
- Kee, R. J., F. M. Rupley, and J. A. Miller (1989). A FORTRAN Chemical Kinetics Package for the Analysis of Gas-Phase Chemical Kinetics. Technical Report SAND89-8009, Sandia National Laboratories, Livermore, CA.
- Kuo, K. K. (1986). *Principles of Combustion*. John Wiley & Sons.
- Law, C. K. (1984). Heat and Mass Transfer in Combustion: Fundamental Concepts and Analytical Techniques. *Prog. Energy Combust. Sci.* **10**, 295–318.
- Law, C. K. and C. J. Sung (2000). Structure, Aerodynamics, and Geometry of Premixed Flamelets. *Prog. Energy Combust. Sci.* **26**, 459–505.
- Lutz, A. E. and Rupley (1994). A FORTRAN Program for Calculating Chemical Equilibrium using Modified Solution Procedure of STANJAN. Technical report, Sandia National Laboratories, Livermore, CA.
- Mason, E. A. and S. C. Saxena (1958). Approximate Formula for the Thermal Conductivity of Gas Mixtures. *Phys. Fluids* **1**, 361–369.

Olikara, C. and G. L. Bowman (1975). A Computer Program for Calculating Properties of Equilibrium Combustion Products with Some Applications to I. C. Engines. *SAE Paper 750468*.

Rogg, B. and W. Wang (1997). RUN-1DL: The Laminar Flame and Flamelet Code. Technical report, Institut für Thermo- und Fluidodynamik.

Strehlow, R. A. (1984). *Combustion Fundamentals*. McGraw-Hill Book Company.

Turns, S. R. (2000). *An Introduction to Combustion: Concepts and Applications* (Second ed.). McGraw-Hill Book Company.

